



UPPSALA
UNIVERSITET



UPTEC W 15028

Examensarbete 30 hp
Juni 2015

Effects of pH and Cation Composition on Sorption of Per- and Polyfluoroalkyl Substances (PFASs) to Soil Particles

Malin Ullberg

ABSTRACT

Effects of pH and Cation Composition on Sorption of Per- and Polyfluoroalkyl Substances (PFASs) to Soil Particles

Malin Ullberg

Per- and polyfluoroalkyl substances (PFASs) have drawn great attention recently, due to their environmental persistence, potential toxicity and global distribution. PFAS is a large family of substances, characterized by a perfluorinated carbon chain and a functional group. All PFASs are synthetic and have been widely used since the 1950s due to their unique properties of being both hydrophobic and oleophobic, making them useful for many industries.

To be able to predict the fate of PFASs in the environment and to obtain detailed understanding of the transport processes, their partitioning behavior between soil particles and water depending on a range of parameters must be investigated. The aims of this study was to investigate the effects of pH, cation composition, functional group and perfluorocarbon chain length on sorption of PFASs to soil particles, by batch sorption experiment in laboratory scale. The laboratory-scale experiments were combined with modelling of the net charge to evaluate if net charge is a good predictor for sorption of PFASs to soil particles.

14 PFASs of varying length and functional groups were studied (PFBA, PFPeA, PFHxA, PFHpA, PFOA, PFNA, PFDA, PFUnDA, PFDoDA, PFTeDA, PFBS, PFHxS, PFOS and FOSA). The effect on sorption of Na^+ , Ca^{2+} (two different concentrations) and Al^{3+} were investigated at pH-range 3-6. Modelling of net charge was carried out in the geochemical model Visual MINTEQ. The soil had 45% organic carbon content.

The adsorption of PFASs was strongly correlated with perfluorocarbon chain length, showing a stronger adsorption to particles with increasing perfluorocarbon chain length (i.e. more hydrophobic). The relation between sorption (represented by the distribution coefficient $\log K_d$) and perfluorocarbon chain length was linear for all PFASs and C_3 to C_{10} PFCAs. The PFASs (sulfonate functional group) sorbed stronger to soil particles than the PFCAs (carboxylic functional group), and FOSA (sulfonamide functional group) sorbed the strongest. For most PFCAs, (C_5 - C_{13}) there was a trend of decreasing $\log K_d$ (i.e. decreased sorption) with increasing pH, due to pH-dependent changes of the soil particle surfaces.

For short and intermediate perfluorocarbon chain length PFCAs (C_5 - C_8) and for PFHxS among the PFASs, cations had a clear effect on sorption. Aluminium ions (trivalent, $\text{Al}(\text{NO}_3)_3$) had the largest effect, followed by calcium (divalent, $\text{Ca}(\text{NO}_3)_2$) where higher concentration resulted in stronger sorption. Sodium (univalent, NaNO_3) had the least influence on sorption.

The net charge modelled with Visual MINTEQ takes into account many parameters (including pH) that affect the surface charge and sorption of PFASs to soil particles. When comparing $\log K_d$ for the different PFASs with pH and net negative charge, net charge was a better predictor of sorption of PFASs to soil particles than solution pH alone.

Keywords: Per- and polyfluoroalkyl substances (PFASs), Soil, Partitioning coefficients, Partitioning, sorption, solution chemistry, electrostatic interaction, Visual MINTEQ

REFERAT

Effekter av pH och katjonsammansättning på sorption av per- och polyfluoralkylsubstanser (PFAS:er) till jordpartiklar

Malin Ullberg

Per- och polyfluoroalkylsubstanser (PFAS:er) har dragit stor uppmärksamhet till sig på senare tid, på grund av deras persistenta egenskaper, potentiella toxicitet och globala utbredning. PFAS är en stor grupp ämnen, kännetecknad av en perfluorinerad kolkedja och en funktionell grupp. Alla PFAS är syntetiska och har använts i stor utsträckning sedan 1950-talet på grund av deras unika egenskaper av att vara både vatten- och fettavstötande, vilket gör dem användbara för många industriella tillämpningar.

För att kunna förutsäga var dessa föroreningars hamnar i miljön och få mer detaljerad förståelse för transportprocesserna, måste deras fördelning beteende mellan jordpartiklar och vatten undersökas för en rad olika parametrar. Syftet med denna studie var att undersöka effekterna av förändrat pH, katjonsammansättning, funktionell grupp och perfluorkolkedjelängd på sorption av PFAS:er till jordpartiklar. Detta gjordes med sorptionsexperiment i laboratorieskala. Laboratorieexperimentet kompletterades med modellering av nettoladdning, för att se huruvida detta väl kunde förklara sorptionen till jordpartiklar.

14 PFAS:er av varierande längd och med tre olika funktionella grupper studerades (PFBA, PFPeA, PFHxA, PFHpA, PFOA, PFNA, PFDA, PFUnDA, PFDODA, PFTEDA, PFBS, PFHxS, PFOS och FOSA). Effekten på sorption av Na^+ , Ca^{2+} (två olika koncentrationer) och Al^{3+} undersöktes vid pH-intervallet 3-6. Modellering av nettoladdning utfördes i den geokemiska modellen Visual MINTEQ. Jorden som användes hade en halt av organiskt kol på 45%.

Adsorptionen av PFAS:er var starkt positivt korrelerad med kedjelängden på de perfluorinerade kolkedjan. Ju längre kolkedja (dvs. mer hydrofob), desto starkare adsorption till partiklar. Relationen mellan sorptionen (här uttryckt som partitioneringskoefficienten $\log K_d$) och kedjelängd var linjär för alla PFSA och för C_3 till C_{10} för PFCA. PFSA (sulfonat) adsorberade starkare än PFCA (karboxyl), och FOSA (sulfonamid) adsorberades starkast. För de flesta PFCA, (C_5 - C_{13}) fanns en allmän trend där $\log K_d$ (dvs. sorption) minskade med ökande pH, på grund av pH-beroende förändringar på jordpartiklarna.

För korta och medellånga PFCA (C_5 - C_8) och för PFHxS hade katjonsammansättningen en tydlig effekt på sorptionen. Aluminiumjoner (trevärd, $\text{Al}(\text{NO}_3)_3$) hade den största effekten, följt av kalcium (tvåvärd, $\text{Ca}(\text{NO}_3)_2$) där den högre koncentrationen resulterade i starkare sorption. Natrium (envärd, NaNO_3) hade minst påverkan på sorptionen till jordpartiklar.

Visual MINTEQ tar hänsyn till många parametrar (inklusive pH), när nettoladdningen på jordpartiklarnas yta räknas ut. När $\log K_d$ för olika PFAS:er jämfördes med endera pH eller negativ nettoladdning, drogs slutsatsen att nettoladdning korrelerade bättre med sorption än pH.

Nyckelord: Perfluoroalkylsubstanser (PFAS), jord, partitioneringskoefficienter, sorption, lösningskemi, elektrostatisk interaction, Visual MINTEQ

ACKNOWLEDGEMENTS

“Why should we tolerate a diet of weak poisons, a home in insipid surroundings, a circle of acquaintances who are not quite our enemies, the noise of motors with just enough relief to prevent insanity? Who would want to live in a world which is just not quite fatal?”

— Rachel Carson, *Silent Spring*

This master thesis of 30 ECTS is the last part of the Master Program in Environmental and Water Engineering at Uppsala University. It has been carried out on the behalf of the Department of Aquatic Science and Assessment at the Swedish University of Agricultural Sciences, SLU. Dan Berggren Kleja, Department of Soil and Environment, Sweden, Geochemistry, acted as supervisor and Lutz Ahrens was the subject reviewer Department of Aquatic Sciences and Assessment. Fritjof Fagerlund at the Department of Earth Sciences at Uppsala University acted as the final examiner.

As this work is coming to an end I would like to express my gratitude to all people involved in the process of creating this thesis. First and foremost I would like to thank my supervisor Dan Berggren Kleja and my subject reviewer Lutz Ahrens for their dedication to my project, for all the support and help throughout my project as well as for always taking the time to answer all my questions. I would also like to thank the staff and the other master students at SLU for being patient and helpful in the lab. Lastly, I would like to thank my flatmates of Kollektivet Näcken, my friends and my family for massaging my shoulders and for making sure I got up every morning, for all the support and for believing in me when I didn't.

Malin Ullberg
Uppsala, 2015

Copyright © Malin Ullberg and the Department of Aquatic Sciences and Assessment, Swedish University of Agricultural Sciences (SLU)
UPTEC W 15028, ISSN 1401-5765. Published digitally at the Department of Earth Sciences, Uppsala University, Uppsala, 2015

POPULÄRVETENSKAPLIG SAMMANFATTNING

Effekter av pH och katjonsammansättning på sorption av per- och polyfluoralkylsubstanser (PFAS:er) till jordpartiklar

Malin Ullberg

Per- och polyfluoroalkylsubstanser (PFAS:er) är en grupp av syntetiska, organiska ämnen som har fått allt större uppmärksamhet den senaste tiden. Dessa ämnen har visat sig vara svårnedbrytbara, giftiga och bioackumulerande, dvs. har en tendens att ansamlas i levande organismer. Det har återfunnits över hela jorden, även på avlägsna platser där inga PFAS:er har tillverkats eller använts på plats. Kunskapen om hur dessa ämnen påverkar människor, djur och natur är fortfarande begränsad, men de misstänks vara bl.a. hormonstörande, cancerogena och ha toxisk påverkan på immunförsvaret.

PFAS är en stor grupp av ämnen, kännetecknad av en molekyl som består av en lång fluorerad kolkedja och en funktionell grupp i ena änden, vilket ger dem den unika egenskapen att de är både vatten- och fettavstötande. De har använts flitigt sedan 50-talet som tensider (ytaktiva ämnen) i många produkter såsom brandsläckningsskum, färg, läder och textilier. I dagsläget är regelverket kring de flesta av dessa ämnen begränsat, och det ämne som fått mest uppmärksamhet inom denna grupp är PFOS. PFOS inkluderades 2009 i Stockholmskonventionens lista över svårnedbrytbara (persistenta) organiska föroreningar (POPs), vilket innebär att användandet och produktionen av PFOS är begränsat sedan dess.

För att kunna förutsäga var dessa föroreningar hamnar i miljön och för att få en mer detaljerad förståelse för hur de rör sig i mark och vatten, måste forskning utföras där viktiga jord- och vattenparametrar varieras. Syftet med denna studie var att variera surhetsgrad (pH), sammansättning av positivt laddade joner (katjoner) och längden på kolkedjan för att se vilken effekt detta hade på sorption av PFAS:er till organiskt material. Med sorption menas hur stor andel av molekylerna som fäster på jordpartiklar snarare än att stanna i vattenfasen. För att göra detta förbereddes olika blandningar av jord, lösning och känd mängd PFASer som sedan analyserades.

Datormodellen Visual MINTEQ användes för att uppskatta hur mycket negativ laddning som fanns på jordprovets yta, vilket är en viktig pusselbit i att förstå hur föroreningarna kommer att bete sig. Det vill säga huruvida de kommer att adsorbera till jord eller stanna i vätskan.

Fjorton PFAS:er av varierande längd studerades (PFBA, PFPeA, PFHxA, PFHpA, PFOA, PFNA, PFDA, PFUnDA, PFDoDA, PFTeDA, PFBS, PFHxS, PFOS och FOSA). Effekten på skillnaden i sorption mellan av natriumjoner, kalciumjoner (två olika koncentrationer) och aluminiumjoner undersöktes över pH-intervallet 3-6 (surt till nära neutralt). Dessa katjoner har olika laddning, och tros därför påverka nettoladdningen olika.

Resultaten visade att adsorptionen av PFAS:er varierade med längden på kolkedjan. Ju längre kolkedja (dvs. mer vattenavstötande), desto starkare adsorberade de till jordpartiklarna i provet. För de flesta av de studerade PFAS:erna fanns ett allmänt samband, där sorptionen minskade med ökande pH. Detta berodde på att ytan på jord-

partiklarna ändrade egenskaper när pH ändrades. Aluminiumjoner hade den starkaste effekten på sorptionen, följt av kalcium, där den högre koncentrationen resulterade i starkare sorption. Natrium hade allra minst påverkan på sorptionen.

Visual MINTEQ tar hänsyn till många parametrar (inklusive pH), när nettoladdningen räknas ut. När sorptionen för olika PFAS:er jämfördes med endera pH eller nettoladdning, drogs slutsatsen att nettoladdning bättre förutsåg sorption än vad pH gjorde.

ABBREVIATIONS

AC	Activated carbon
BC	Oil-derived black carbon
C _x	Fluorocarbon chain of length x
DOC	Dissolved organic carbon
FASAs	Perfluoroalkyl sulfonamides
F _{oc}	Fraction organic carbon
FOSA	Perfluorooctane sulfonamide
HPLC-MS/MS	High-performance liquid chromatography coupled with tandem mass spectrometry
IS	Internal standard
K _d	Soil-water distribution coefficient
K _{oc}	Organic carbon normalised partition coefficient
PFASs	Per- and polyfluoroalkyl substances
PFBA	Perfluorobutanoate
PFBS	Perfluorobutane sulfonic acid
PFCAs	Perfluorinated carboxylate acids
PFDA	Perfluorodecanoate
PFDoDA	Perfluorododecanoate
PFHpA	Perfluorohepanoate
PFHxA	Perfluorohexanoate
PFHxS	Perfluorohexane sulfonic acid
PFNA	Perfluorononanoate
PFOA	Perfluorooctanoate
PFOS	Perfluorooctane sulfonic acid
PFPeA	Perfluoropentanoate
PFSA	Perfluorinated sulfonic acids
PFTeDA	Perfluorotetradecanoate
PFUnDA	Perfluoroundecanoate
POPs	Persistent organic pollutants
PP	Polypropylene
SD	Standard deviation
SPE	Solid phase extraction
SPM	Suspended particulate matter
S _w	Water solubility

TABLE OF CONTENTS

ABSTRACT	II
ACKNOWLEDGEMENTS	IV
POPULÄRVETENSKAPLIG SAMMANFATTNING	V
ABBREVIATIONS	VII
1. INTRODUCTION	1
1.1. OBJECTIVES AND HYPOTHESIS	1
2. BACKGROUND	2
2.1. PER- AND POLYFLUOROALKYL SUBSTANCES (PFASs)	2
2.1.1. Production and usage	2
2.1.2. Toxicity and occurrence in humans and wildlife.....	4
2.1.3. Regulations	4
2.2. PARTITIONING BEHAVIOR OF PFASs	5
2.2.1. Physiochemical properties	5
2.2.2. Influence of chain length and functional group	5
2.2.3. Influence of organic carbon	6
2.2.4. Influence of pH	7
2.2.5. Influence of anions and cations	7
2.2.6 Acid dissociation constants, pK_a	8
3. MATERIAL AND METHODS	8
3.1. EXPERIMENT SETUP	8
3.2. SOIL CHARACTERISTICS	8
3.3. PFAS SPIKING SOLUTION	8
3.4. BATCH SORPTION EXPERIMENT	9
3.4.1. Pilot experiment.....	9
3.4.2. Main experiment.....	10
3.5. CHEMICAL ANALYSES	11
3.5.1. PFAS analysis	11
3.5.2. pH	13
3.5.3. Dissolved organic carbon	13
3.5.4. Quality assurance/quality control (QA/QC).....	13
3.6. MODELLING OF NET CHARGE USING VISUAL MINTEQ	13
3.7. DATA ANALYSIS	14
4. RESULTS	15
4.1. BATCH SORPTION EXPERIMENT	15
4.1.1. PFCAs.....	15
4.1.2. PFASs and FOSA	17
4.2. INFLUENCE OF CARBON CHAIN LENGTH AND FUNCTIONAL GROUPS ON SORPTION OF PFASs TO SOIL	18
4.3. INFLUENCE OF CATIONS, PH AND NET NEGATIVE CHARGE ON SORPTION OF PFASs TO SOIL	20
4.3.1. Influence of cations and pH on sorption of PFASs to soil	20
4.3.2. Influence of cations and net negative charge on sorption of PFASs to soil	21
5. DISCUSSION	26
5.1. BATCH SORPTION EXPERIMENTS	26

5.2. INFLUENCE OF CARBON CHAIN LENGTH AND FUNCTIONAL GROUPS ON SORPTION OF PFASs TO SOIL	26
5.3. INFLUENCE OF CATIONS, PH AND NET NEGATIVE CHARGE ON SORPTION OF PFASS TO SOIL.....	27
5.3.1. Influence of pH.....	27
5.3.2. Influence of cations.....	28
5.3.3. Influence of net negative charge.....	28
5.3.4. Comparison between pH and net negative charge.....	28
5.4. FUTURE PERSPECTIVES	29
6. CONCLUSION	29
7. REFERENCES.....	31
APPENDIX.....	34
Appendix I	34
Appendix II.....	35
Appendix III	36
Appendix IV.....	36
Appendix V	37
Appendix VI.....	38
Appendix VII	39

1. INTRODUCTION

Per- and polyfluoroalkyl substances (PFASs) have drawn great attention recently, due to their environmental persistence, potential toxicity and global distribution (Ahrens et al., 2011; Du et al., 2014). PFAS is a large family of substances, characterized by a perfluorinated carbon chain and a functional group. All PFASs are anthropogenic and have been widely used since the 1950s due to their unique properties of being both hydrophobic and oleophobic, making them useful for many industries (Borg and Håkansson, 2012).

In Sweden, PFASs have been found in human blood in worrisome levels, raising a lot of concern. The likely pathway of exposure is drinking water, where the water source have been contaminated by fire extinguishing foam utilized at fire practicing areas (Glynn et al., 2013; Hedenberg, 2014; Ny Teknik, 2014).

To be able to predict the fate of PFASs in the environment, to obtain a detailed understanding of the transport processes, their partitioning behavior between soil particles and water depending on a range of parameters must be investigated. Even though there has been a great interest for PFASs in the research community over the last 20 years or so, there is still a lot that is unknown.

1.1. OBJECTIVES AND HYPOTHESIS

The aims of this study was to investigate the effects of pH, cation composition (particularly trivalent cation Al^{3+}), functional group and perfluorocarbon chain length on sorption of PFASs to soil particles, by batch sorption experiments at laboratory scale. The laboratory-scale experiments were combined with modelling of the soil surface net charge to evaluate if net charge is a good predictor for sorption of PFASs to soil particles.

Previous research has studied effects on sorption by cations with valence two or less (e.g. Na^+ , Ca^{2+} and Mg^{2+}), whereas the knowledge of the effect of trivalent cations (such as Al^{3+}) is limited. The concept of correlating sorption with modelled surface net charge is previously uninvestigated. This study covers a greater range of PFASs than most previous studies.

The main hypotheses to be investigated were that:

- sorption of PFASs to organic matter is a balance between two counteracting forces: firstly attraction forces between the hydrophobic ‘tail’ of PFASs and hydrophobic parts of soil organic matter and secondly repulsion forces between the negatively charged ‘head’ (functional group) of the PFASs molecules and the negatively charged carboxylic groups of soil organic matter.
- the hydrophobic attraction forces between PFASs and organic matter would increase with increased carbon chain length of the PFASs molecule.
- the repulsion forces would decrease when the charge of carboxylic groups of the soil surface decreases due to either protonation or complex formation with Ca^{+2} or Al^{3+} -ions.
- the net charge effect could be modelled using geochemical model Visual MINTEQ and that the modelled net charge of the soil would be a better predictor of sorption than pH.

2. BACKGROUND

2.1. PER- AND POLYFLUOROALKYL SUBSTANCES (PFASs)

Per- and polyfluoroalkyl substances (PFASs) is a collective term for a large group of synthetic highly fluorinated organic compounds that has been produced and used for industry purposes for over 50 years. As highly persistent environmental contaminants, PFASs have been found over the whole globe in humans, wildlife and in the environment (Borg and Håkansson, 2012). Many studies have focused on perfluorooctane sulfonic acid (PFOS) and perfluorooctanoate (PFOA) which are two out of many PFASs, (e.g. Ahrens et al., 2011; Chen et al., 2009, 2009; Du et al., 2014; Pan et al., 2009; Pan and You, 2010; Senevirathna et al., 2010; Zareitalabad et al., 2013) especially during earlier years, although newer research cover a wider spectrum of PFASs (Ahrens et al., 2010; Kim et al., 2015; Labadie and Chevreuil, 2011; Post et al., 2013).

The general structure is a polyfluoroalkyl chain, typically three to fifteen carbons long, where fluorine replaces the hydrogen, with a functional group at one end (Borg and Håkansson, 2012). For a fully perfluorinated compound, the molecular structure is $(C_nF_{2n+1})^{-1}$ (Buck et al., 2011). The stable and strong saturated carbon-fluorine bond creates a main structure of PFASs that is both thermally and chemically stable as well as resistant to chemical, physical and biological degradation (Buck et al., 2011; Giesy and Kannan, 2002; Rahman et al., 2014)

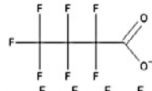
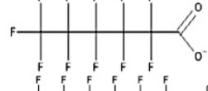
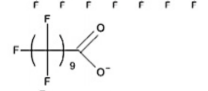
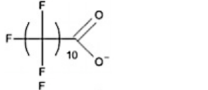
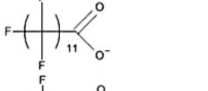
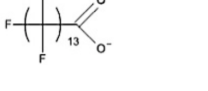
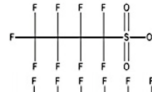
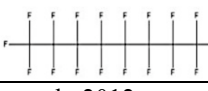
For this particular study, fourteen PFASs with varying chain lengths and functional groups were studied. Table 1 show the acronyms, the molecular structure, the different functional groups studied, the molar weight (divided by the subgroups PFCAs, PFASs and FASAs), the water solubility (S_w) and the acid dissociation constant (pK_a) of the studied compounds.

2.1.1. Production and usage

A large number of PFASs have been commercially produced for over 50 years, for example as surfactants (Borg and Håkansson, 2012; Buck et al., 2011; Giesy and Kannan, 2002), or as processing aid for fluoropolymers (Buck et al., 2011). Contrary to traditional surfactants, that are comprised by a water-soluble hydrophilic part and a water-insoluble hydrophobic part, the fluorinated carbon chain of PFASs is both oil- and water repellent, making them especially useful in many industrial areas. Such industrial uses include surface protection for paper and packaging, water-proofing and stain and oil repellent of different textiles (Borg and Håkansson, 2012).

Further, PFASs have been used in insecticides, fire-fighting foams, ski-waxes and hydraulic fluids in airplanes (Ahrens et al., 2011; Borg and Håkansson, 2012; Glynn et al., 2013; Moody et al., 2003). Since 2002, when the most commonly used PFOA and PFOS was phased out, shorter-chained PFASs like perfluorobutanoate (PFBA) have successively replaced them (Buck et al., 2011). There is no production of PFASs in Sweden, and has not been, so the sources is likely a combination of emission from industries using these compounds, leachate from landfills and from sewage treatment (Borg and Håkansson, 2012).

Table 1. List of the PFASs analyzed in this study along with their molecular structure (Borg and Håkansson, 2012), molecular weight (MW), the water solubility ($\log S_w$) and acid dissociation constant (pK_a).

Compound	Acronym	Structure	Chemical formula	MW (g mol ⁻¹)	Log S _w (mol L ⁻¹)	pK _a
Perfluorobutanoate	PFBA		C ₃ F ₇ COOH	213.04	0.76 ^b	0.05 ^c
Perfluoropentanoate	PFPeA		C ₄ F ₉ COOH	263.05	1.45 ^b	-0.10 ^c
Perfluorohexanoate	PFHxA		C ₅ F ₁₁ COOH	313.06	2.15 ^b	-0.17 ^c
Perfluoroheptanoate	PFHpA		C ₆ F ₁₃ COOH	363.07	2.85 ^b	-0.2 ^c
Perfluorooctanoate	PFOA		C ₇ F ₁₅ COOH	413.08	3.55 ^b	-0.22 ^c
Perfluorononanoate	PFNA		C ₈ F ₁₇ COOH	463.09	4.24 ^b	-0.22 ^c
Perfluorodecanoate	PFDA		C ₉ F ₁₉ COOH	513.10	4.94 ^b	-0.22 ^c
Perfluoroundecanoate	PFUnDA		C ₁₀ F ₂₁ COOH	563.11	5.62 ^b	-0.22 ^c
Perfluorododecanoate	PFDoDA		C ₁₁ F ₂₂ COOH	613.12	5.80 ^b	-0.22 ^c
Perfluorotetradecanoate	PFTeDA		C ₁₃ F ₂₂ COOH	713.14	7.05 ^b	-0.22 ^c
Perfluorobutane sulfonic acid	PFBS		C ₄ F ₉ SO ₃ H	300.12	1.15 ^b	0.14 ^c
Perfluorohexane sulfonic acid	PFHxS		C ₆ F ₁₃ SO ₃ H	400.14	2.91 ^b	0.14 ^c
Perfluorooctane sulfonic acid	PFOS		C ₈ F ₁₇ SO ₃ H	500.16	4.30 ^b	0.14 ^c
Perfluorooctane-sulfonamide	FOSA		C ₈ F ₁₇ SO ₂ NH ₂	499.18	4.33 ^b	6.56 ^c

^aKim et al., 2015, ^bWang et al., 2011, ^cAhrens et al., 2012

2.1.2. Toxicity and occurrence in humans and wildlife

There are concerns about the toxicity of PFASs for humans and wildlife, and the number of studies on the subject is growing steadily, again with an emphasis on PFOA and PFOS (Hansen et al., 2001; Kannan et al., 2004), where PFOS has been officially classified as a persistent, bioaccumulative, and toxic substance (Buck et al., 2011). PFCAs, such as PFOA and perfluorodecanoate (PFDA), have potential to affect enzymes and proteins involved in lipid metabolism and other toxic effects, including accumulation of triglycerides in liver and reduction of thyroid hormone (Giesy and Kannan, 2002). Contrary to other studied persistent organic contaminants, PFASs does not accumulate in fatty tissues, but rather to proteins in liver, blood and eggs (Kannan et al., 2004). However, there is a large difference in the toxicity and health problems among the studied PFASs, and among PFCAs, the toxic effects vary depending upon carbon chain length (Giesy and Kannan, 2002). For example, the potencies of PFCAs to induce peroxisomal beta-oxidation increased with increased carbon chain length (Kudo et al., 2000). Several studies have measured levels in PFASs in human blood, over time (Glynn et al., 2012, 2007; Hansen et al., 2001; Kannan et al., 2004; Kärman et al., 2006). Glynn et al. (2012) concluded that increasing trends in PFASs concentration in human serum over time was observed for perfluorobutane sulfonic acid (PFBS), perfluorohexane sulfonic acid (PFHxS), perfluorononanoate (PFNA) and PFDA, whereas decreasing trends was observed for PFOS, perfluorooctane sulfonamide (FOSA) and PFOA, which could be connected to the phasing-out of these compounds (Borg and Håkansson, 2012). In the environment, PFASs have the potential to bioaccumulate in fish (Martin et al., 2003), rendering this a possible exposure risk for humans, and show up in high concentrations in top predators such as otter, mink, polar bear and seal (Giesy and Kannan, 2002).

2.1.3. Regulations

The Swedish Chemical Agency (Kemikalieinspektionen) has reported PFASs as compounds with especially hazardous characteristics (Glynn et al., 2013). However, risk assessments for many of them are either lacking or require improvement (Borg and Håkansson, 2012). PFOS has been included in the Stockholm Convention on Persistent Organic Pollutants (POPs) and therefore been globally restricted in its use (Ahrens et al., 2011). PFOS and PFOA are also regulated in its use in Germany as well as in the United States and Canada, although some specific applications are still allowed (Du et al., 2014). These restrictions have resulted in development of new PFASs with similar characteristics (Ahrens et al., 2011; Rahman et al., 2014).

There are no general enforced guidelines for concentrations of PFASs in drinking water in either Sweden or Europe, however target values on PFOS at 350 to 1 000 ng L⁻¹ in drinking water has been set up by The Swedish Environmental Protection Agency (Naturvårdsverket). The interval is based upon tolerable daily intake, body weight and intake of drinking water (Glynn et al., 2013). The Swedish National Food Agency (Livsmedelsverket) has stated preliminary guidelines regarding PFBS, PFHxS, PFOS, perfluoropentanoate (PFPeA), perfluorohexanoate (PFHxA), perfluoroheptanoate (PFHpA) and PFOA, that the sum of the seven PFASs should not exceed 90 ng L⁻¹ in drinking water and also be below the tolerable daily intake (TDI) guideline of 900 ng L⁻¹ in drinking water (Livsmedelsverket, 2015). More research on exposure and toxicology of PFASs is required to make better risk assessments in the future (Rahman et al., 2014).

2.2. PARTITIONING BEHAVIOR OF PFASs

2.2.1. Physicochemical properties

The nature of the structure of the PFASs gives them a set of properties that makes them unique. The physicochemical properties of PFASs, and how they behave in the environment depends on their perfluorocarbon chain length and on their functional group. Further this particular structure gives them water and oil repellent properties as well as resistance to oxidation (Buck et al., 2011). Three subgroups of PFASs are studied in this report, ten perfluoroalkyl carboxylates (PFCAs), three perfluoroalkyle sulfonates (PFSAs) and one perfluorooctane sulfonamide (FOSA). The subgroups can be categorised as either long-chained (for PFCAs seven or more perfluorinated carbons, and for PFSAs six or more) or short-chained (Buck et al., 2011). As a general rule, the polarity and solubility in water (S_w) increases with a decreasing carbon chain length (Table 1). PFCAs and PFSAs are considered stable end products that won't degrade under naturally occurring conditions (Borg and Håkansson, 2012).

Being surfactants, PFASs have the possibility of forming micelles and hemi-micelles. However, both Johnson et al. (2007) and Higgins and Luthy (2006) states that there is little potential of micelle formation or even hemi-micelles forming within the sediment organic matter.

2.2.2. Influence of chain length and functional group

Sorption behavior and bioaccumulation of PFCAs and PFSAs is strongly influenced by molecular structure, where longer chained PFASs adsorb more strongly to organic matter, with a near linear relation between sorption (presented as the organic carbon normalized partitioning coefficient $\log K_{oc}$) and the perfluoroalkyl chain length (Labadie and Chevreuil, 2011). Higgins and Luthy (2006) found that on average, the sorption of the PFASs was 1.7 times stronger (0.23 log units) than for the PFCAs, and that although both chain length and functional group impact the sorption, chain length is the dominating structural feature concerning adsorption to sediment materials and suspended particulate matter (SPM), a conclusion that also Ahrens et al. (2010) found (0.71–0.76 log units higher for PFSAs). The highest particulate associated fraction observed in that study was for perfluoroundecanoate (PFUnDA) with 62%. The organic carbon normalized partition coefficient, K_{OC} , for individual PFASs from a number of studies is presented in Table 2.

Ahrens et al. (2010) found that short-chained PFCAs were exclusively detected in the dissolved phase whereas long-chained PFCAs, PFSAs and FOSA bound more strongly to particles and that the sorption was influenced by the soil organic carbon content. In general, PFSAs, FOSA and long-chained PFCAs have a stronger potential to interact with SPM, thus these PFASs have a higher potential for sedimentation and accumulation in sediments (Ahrens et al., 2010). PFASs molecules may prefer adsorption onto solid surfaces rather than staying in water phase even if the adsorbent surfaces are hydrophobic due to their hydrophobic and oleophobic properties (Du et al., 2014). The electrostatic negativity is principally originated from the functional head of the compound, while the tail of the molecule mostly displays the hydrophobic effect which is overwhelming the charged effect (Du et al., 2014).

Table 2. Log K_{OC} with standard deviation for Ahrens et al., 2011, 2010; Higgins and Luthy, 2006 and Labadie and Chevreuil, 2011.

[mL g ⁻¹]	Log K_{OC} ± SD Higgins and Luthy, 2006 ^a (n)	Log K_{OC} ± SD Ahrens et al., 2011 ^b (n)	Log K_{OC} ± SD Ahrens et al., 2010 ^c (n)	Log K_{OC} ± SD Labadie and Chevreuil, 2011 ^d (n)
PFHxA				2.1 ± 0.2 (3)
PFHpA			2.9 ± 0.0 (6)	2.1 ± 0.2 (3)
PFOA	2.1 ± - (2)	2.4 ± 0.2 (9)	3.5 ± 0.1 (6)	
PFNA	2.4 ± 0.1 (3)		4.0 ± 0.1 (6)	2.9 ± 0.1 (3)
PFDA	2.8 ± 0.1 (5)		4.6 ± 0.1 (6)	3.8 ± 0.2 (3)
PFUnDA	3.3 ± 0.1 (5)		5.1 ± 0.1 (6)	4.7 ± 0.1 (3)
PFDoDA				5.6 ± 0.2 (3)
PFHxS			3.7 ± 0.3 (6)	2.2 ± 0.1 (3)
PFOS	2.6 ± 0.1 (4)	3.5 ± 0.9 (18)	4.8 ± 0.1 (6)	3.7 ± 0.2 (3)
FOSA		4.2 ± 1.0 (22)	4.5 ± 0.1 (6)	

^a Organic carbon content in sediment ranging from 0-10%.

^b Organic carbon content in sediment ranging from 0-1.6 %

^c Organic carbon content in sediment ranging from 1.5-10.6 %.

^d Organic carbon content in sediment 4.8%

n = number of samples included in the calculation

2.2.3. Influence of organic carbon

Several studies have found presence of organic matter to be an important factor to the partitioning behavior of PFASs in soil (Ahrens et al., 2011; Chen et al., 2009; Du et al., 2014; Higgins and Luthy, 2006; Milinovic et al., 2015; You et al., 2010). Higgins and Luthy (2006) concluded that the dominant sediment parameter influencing sorption of anionic PFASs was organic carbon in sediment. Ahrens et al. (2011) also found that the level of organic content had a significant influence on the partitioning, whereas for sediment with little or no organic content, the density of the sediment became the most important factor. According to Higgins and Luthy (2006), organic carbon levels in sediment, rather than sediment iron oxide content, was the dominant sediment parameter affecting sorption, pointing at the importance of hydrophobic interactions.

For individual PFASs, Milinovic et al. (2015) found that sorption, calculated as soil-water distribution coefficient (K_d) increased linearly with increasing organic matter in the soil and suggested therefore that the main sorption mechanism of PFASs is based predominantly on interactions between the hydrophobic fluorocarbon chain of the compound and the organic matter. Similar correlation for PFOS was found by Du et al. (2014), who further stated that the functional groups on the surface and the pore structure of the adsorbents plays an important role in the adsorption.

Chen et al. (2009) studied how pH and Ca²⁺ concentration affected sorption of PFOS to oil-derived black carbon (BC) and found that hydrophobic interactions of the hydrophobic moieties of PFOS with oil played a dominant role. BC sorption for PFOS was not stronger than other natural organic carbon in the case of low Ca²⁺ concentration and pH 5.05.

Given its large influence in sorption behavior of PFASs, activated carbon (AC) is the most widely used adsorbent for water treatment (Du et al., 2014). The high removal

efficiency of AC is due to the large surface, which is generally non-polar with few functional groups, rendering it suitable for removing hydrophobic pollutants. For example, the removal efficiency of PFOS from wastewater was 99% using granular AC (Du et al., 2014). The adsorption kinetics of PFASs onto the AC have been found to be closely related to the particle diameter and pore size of adsorbents, with powdered adsorbents having fast adsorption while the granular adsorbents normally show very slow adsorption for PFOS (Du et al., 2014).

2.2.4. Influence of pH

Many studies have demonstrated the importance of pH when it comes to sorption behavior of PFASs (e.g. Chen et al., 2009; Du et al., 2014; Higgins and Luthy, 2006; Tang et al., 2010; Wang et al., 2012), but the theories to why it matters are diverse. The effects are typically described as due to protonation or deprotonation of the organic acids near its pK_a , but there are likely other processes at play (Higgins and Luthy, 2006). It is likely that pH effects are due to pH-dependent changes in the sorbent, such as surface charge of organic matter, rather than protonation/deprotonation of the sorbate (Higgins and Luthy, 2006). In the same study, there was a significant drop in the observed K_d for the most hydrophobic (long-chained) compounds at high pH (7.5) which likely corresponds to the increased DOC concentration (Higgins and Luthy, 2006). Wang et al. (2012) suggests that the decrease in PFOS and PFOA adsorption with increasing pH is due to an increase in ligand exchange reactions and decrease of electrostatic interactions, which is also supported by results from Higgins and Luthy (2006). Also Chen et al. (2009) reports pH dependence and states it is likely that the pH effects are due to pH-dependent changes in sorbent rather than protonation/deprotonation of the sorbate.

With the increase of pH, adsorbent surfaces tend to become more negatively charged (or less positively charged) via the protonation and deprotonation of some surface functional groups, leading to stronger electrostatic repulsion for anionic PFASs. In contrast, increasing concentration of ions can compress the electrical double layers of sorbents, which weakens not only the electrostatic interactions (attraction or repulsion) between sorbent surfaces and PFAS molecules but also the electrostatic repulsion between the anionic PFASs themselves (Du et al., 2014).

2.2.5. Influence of anions and cations

As stated in 2.2.4. Influence of pH, sorption of PFASs changes with pH. However, when a sufficient amount of divalent cations are present in solution, the influence of pH changes (Chen et al., 2009; Du et al., 2014; Tang et al., 2010; You et al., 2010). This has been reported for Ca^{2+} and Mg^{2+} and is due to the fact that adsorbent surfaces develop more basic sites to bind divalent cations when pH increases. The potential mechanisms behind these results are increased sorption of PFASs by divalent cation bridging effect between perfluorochemicals, salting-out, competitive adsorption with inorganic anions and electrical double layer compression (Du et al., 2014; Wang et al., 2012). Results from You et al. (2010) showed that the sorption of PFOS onto sediment increased threefold as the Ca^{+2} concentration increased from 0.005 to 0.5 M at pH 7.0, and nearly sixfold at pH 8.0.

Higgins and Luthy (2006) showed that Na^+ has little or no effect on sorption although the experiment were conducted with similar ranges of ionic strength as Ca^{2+} , and that implies that the observed changes are not simply ionic strength (Higgins and Luthy,

2006). Higgins and Luthy (2006) interpreted the effects of Ca^{2+} on sorption as a reduction in the charge present on the organic matter.

In an sorption experiment with PFOS and BC, Chen et al. (2009) found similar conclusions, and explained the results as the screening effect when Ca^{2+} partially neutralizes the negative surface charge by specific interactions between the functional groups present in the BC and Ca^{2+} resulting in an increase in the attractive forces between the surface of the BC and the anionic PFOS and in turn resulted in an increase in sorption.

The effect on trivalent ions, such as Al^{3+} , on sorption has yet not been investigated thoroughly, but it has potential to affect sorption even stronger than the divalent ions because it has a higher potential of neutralizing the negatively charged surface of the organic matter and therefore decrease the repulsive effect of the negatively charged PFASs.

2.2.6 Acid dissociation constants, pK_a

Both PFCAs and PFSAs are relatively strong acids, where PFSAs are stronger, and tend to dissociate to anionic form in the pH range of most natural systems (Rayne and Forest, 2009). The pK_a value describes the tendency of an acid to dissociate to its conjugate acid-base pair, with a low pK_a meaning that a compound has a stronger tendency to dissociate to its conjugate ions (Rayne and Forest, 2009). pK_a for the compounds in this study are -0.22–0.05 for PFCAs, 0.14 for PFSAs and 6.65 for FOSA (Table 1).

3. MATERIAL AND METHODS

3.1. EXPERIMENT SETUP

To study the influence of pH, and cation concentration on sorption of PFASs to organic matter, known concentrations of sodium-, calcium- and aluminium nitrate respectively were added to an organic soil along with different ratios of acid and base to create an adequate pH-range. A pre-test of nine samples was designed to establish additions for adequate acid-base equilibrium. Before shaking, the samples were spiked with the 14 different PFASs.

3.2. SOIL CHARACTERISTICS

The soil was a mor sample with high carbon content from a spodosol and was collected in 2011 in central Sweden (Risbergshöjden, 59°43'00"N15°01'59"E), and since then kept refrigerated in its field-moist state (Gustafsson et al., 2014a). The soil was sieved through a 2 mm sieve to remove roots and larger particles. The water content was at the time of this study 66%, determined by drying in a 105°C oven for 24h.

Gustafsson et al. (2014) determined the concentrations of geochemically active Al, Ca, Cr, Fe, K, Mg, Mn and Cr (Appendix I). Carbon and nitrogen content were 45 % and 1.3% respectively, on dry-weight basis.

3.3. PFAS SPIKING SOLUTION

Equimolar stock solution of 14 PFASs solved in methanol ($c = 5 \mu\text{g/mL}$) of PFBA, PFPeA, PFHxA, PFHpA, PFOA, PFNA, PFDA, PFUnDA, perfluorododecanoate (PFDoDA), perfluorotetradecanoate (PFTeDA), PFBS, PFHxS, PFOS and FOSA (Table 1) was purchased from Sigma-Aldrich. Internal standards (IS) for the PFASs

included the mass labeled compounds $^{13}\text{C}_4\text{PFBA}$, $^{13}\text{C}_2\text{PFHxA}$, $^{13}\text{C}_4\text{PFOA}$, $^{13}\text{C}_5\text{PFNA}$, $^{13}\text{C}_2\text{PFDA}$, $^{13}\text{C}_2\text{PFUnDA}$, $^{13}\text{C}_2\text{PFDoDA}$, $^{18}\text{C}_2\text{PFHxS}$, $^{13}\text{C}_4\text{PFOS}$, M_8FOSA , $\text{d}_3\text{-N-MeFOSAA}$, $\text{d}_5\text{-N-EtFOSAA}$, $\text{d}_3\text{-N-MeFOSA}$, $\text{d}_3\text{-N-EtFOSA}$, $\text{d}_7\text{-N-MeFOSE}$ and $\text{d}_9\text{-N-EtFOSE}$, all purchased from Wellington Laboratories (purity 99%).

3.4. BATCH SORPTION EXPERIMENT

3.4.1. Pilot experiment

The desired pH for the main experiment was pH 3, 4, 5 and 6. To determine adequate additions of HNO_3 and NaOH to achieve these values, the chemical equilibrium model Visual MINTEQ was used (Gustafsson, 2013). To confirm the output from the model, a pilot batch experiment of nine samples was conducted. These samples were not spiked with PFASs standard.

Solution

To vary the cation concentration, different volumes of dissolved nitrate salts were added to the solution (Table 3). 30 mM NaNO_3 , 30 mM $\text{Ca}(\text{NO}_3)_2$, 20 mM $\text{Al}(\text{NO}_3)_3$ solutions were prepared in volumetric flasks using Millipore-water. NaNO_3 were added to all samples to keep the nitrate concentration constant. Three series of samples were prepared with final concentration 10 mM NaNO_3 , 3 mM $\text{Ca}(\text{NO}_3)_2$ and 2 mM $\text{Al}(\text{NO}_3)_3$ respectively. Concentrations were chosen to reflect naturally occurring levels in soil water, and within the same range as earlier studies (Chen et al., 2009; Higgins and Luthy, 2006). To vary pH in the solution, different volumes (Table 3) of 20 mM HNO_3 and 20 mM NaOH solutions were added, prepared with Millipore water (Millipak, 0.22 μm filter) in volumetric flasks.

Table 3. Amounts (mL) of acid, base and nitrate salts added to the different samples in the pilot batch experiment.

[mL]	30 mM NaNO_3	20 mM HNO_3	20 mM NaOH	30 mM $\text{Ca}(\text{NO}_3)_2$	20 mM $\text{Al}(\text{NO}_3)_3$	H_2O	Modelled pH	Measured pH
Sodium								
Na a	10	6	0	0	0	14	2.6	2.7
Na b	10	0	3	0	0	17	4.7	4.7
Na c	10	0	9	0	0	11	6.6	6.0
Calcium								
Ca a	4.0	3.0	0	3.0	0	20	2.9	2.9
Ca b	4.0	0	6.0	3.0	0	17	4.7	4.6
Ca c	4.0	0	11	3.0	0	13	6.3	5.7
Aluminium								
Al a	4.0	1.5	0.0	0	3.0	22	2.8	2.7
Al b	4.0	0	9.0	0	3.0	14	4.7	4.7
Al c	4.0	0	14	0	3.0	9.5	6.3	5.7

Addition of soil

1.0 g of soil was added to each of the 50 mL polypropylene (PP) tubes (Corning 430290 50 mL centrifuge tube, non-pyrogenic polypropylene), to which 30 mL of solution containing acid/base, cations and Millipore water was added, resulting in a liquid to solid ratio of 91 mL g⁻¹.

Handling of samples

According to Higgins and Luthy (2006), shaking for 7-days is sufficient to reach equilibrium. The nine samples were sealed and mounted laying down on a horizontal shaker (Gerhardt), set to 133 rpm and left for 7 days (168h). Immediately after shaking was finished, the samples were centrifuged (Eppendorf Centrifuge 5810) for 20 min at 3000 rpm and pH measured.

3.4.2. Main experiment

Acid-base equilibrium

A combination of model output and measured pH (Table 3) from the pilot batch experiment was used to come up with the additions of HNO₃ and NaOH for the main experiment, presented in Table 4, using same prepared stock solutions as above.

Addition of cations

Four series of samples were prepared with final concentrations of 10 mM NaNO₃, 3 mM Ca(NO₃)₂ (low concentration), 5 mM Ca(NO₃)₂ (high concentration) and 2 mM Al(NO₃)₃ respectively (Table 4), using same prepared stock solutions as above.

Addition of soil

1.33 g of soil was added to each of the 50 mL PP tubes, to which 40 mL of solution containing acid/base, cations and Millipore water was added, resulting in a liquid to solid ratio of 91 mL g⁻¹.

Spiking

The PFASs standard was added to the samples before shaking using a disposable 10 µL glass pipette. This resulted in a theoretical initial aqueous concentration of 1248 ng L⁻¹ of each compound or 50 ng per 40 mL sample.

Handling of samples

As for the pilot batch experiment, spiked samples were sealed and mounted laying down on a horizontal shaker set to 133 rpm and left for 7 days (168h). Immediately after shaking was finished, the samples were centrifuged for 20 min at 3000 rpm and the liquid decanted into new rinsed PP tubes and stored in a refrigerator until further analysis. The samples of the main experiment were prepared in duplicates, along with positive (PFASs spike in Millipore water, no soil) and negative (Millipore water) controls. In total 36 samples were prepared, of which 32 contained soil.

Table 4. Amounts (mL) of acid, base, water and Na⁺, Ca²⁺ and Al³⁺ solutions added to the different samples. The pH stated is the target value.

[mL]	30 mM NaNO ₃	20 mM HNO ₃	20 mM NaOH	30 mM Ca(NO ₃) ₂	20 mM Al(NO ₃) ₃	H ₂ O (Millipore)
Sodium						
Na pH 3	13	4.0	0	0	0	23
Na pH 4	13	0	2.0	0	0	25
Na pH 5	13	0	6.0	0	0	21
Na pH 6	13	0	12	0	0	15
Calcium low concentration						
Ca pH 3 [3 mM]	5.3	4.0	0	4.0	0	27
Ca pH 4 [3 mM]	5.3	0	4.0	4.0	0	27
Ca pH 5 [3 mM]	5.3	0	10	4.0	0	21
Ca pH 6 [3 mM]	5.3	0	15	4.0	0	16
Calcium high concentration						
Ca pH 3 [5 mM]	5.3	4.0	0	6.7	0	24
Ca pH 4 [5 mM]	5.3	0	4.0	6.7	0	24
Ca pH 5 [5 mM]	5.3	0	10	6.7	0	18
Ca pH 6 [5 mM]	5.3	0	15	6.7	0	13
Aluminium						
Al pH 3	5.3	0	0	0	4.0	31
Al pH 4	5.3	0	10	0	4.0	21
Al pH 5	5.3	0	14	0	4.0	17
Al pH 6	5.3	0	20	0	4.0	11
Controls						
Negative (water)	0	0	0	0	0	40
Positive (water + PFASs)	0	0	0	0	0	40

3.5. CHEMICAL ANALYSES

3.5.1. PFAS analysis

Due to limited time and resources, only the liquid phase was analysed for PFAS content, with the presumption that the difference between added known concentration of PFASs and the measured concentration of the liquid phase accurately enough reflects the sorbed PFAS concentration.

Preparation of samples

All samples were filtered through multiple 0.45 µm syringe filters (VWR International 25 mm syringe filters, nylon and polypropylene), all rinsed thrice with methanol. 10 mL (measured by weight) sample was spiked with 100 µL internal standard (PFAS IS) using automatic micro-pipette, in order to correct for any potential losses of PFASs during the extraction and the following concentration.

Solid phase extraction for the filtrated water

Solid phase extraction (SPE) WAX cartridges (Oasis WAX 6cc Cartridge, 150 mg, 30 µg) were prepared for extraction by passing through 4 mL ammonium hydroxide in methanol (0.1 %), followed by 4 mL methanol and 4 mL Millipore water, before loading with the samples which passed through by gravity (Figure 1). Lastly, 4 mL of buf-

fer solution (25 mM ammonium acetate, pH 4) concluded the extraction phase. The cartridges were then dried in centrifuge, at 3000 rpm for two minutes.



Figure 1. Samples loaded into SPE cartridges mounted to a manifold.

Elution

At this point all PFASs were sorbed to the resin material in the cartridges. Elution was carried out by passing first 4 mL of methanol and then 4 mL of ammonium hydroxide in methanol (0.1 %) into 15 mL PP tubes first rinsed with methanol.

Concentration

In order to concentrate the samples down to the final volume of 1 mL, evaporation by nitrogen gas was used (N-EVAP 112, Nitrogen Evaporator from Organomation Associates Inc.). The concentrated liquid was transferred to small brown glass vials using disposable glass pipettes and reduced to 1 mL (Figure 2). The samples were stored in a freezer until analysis.

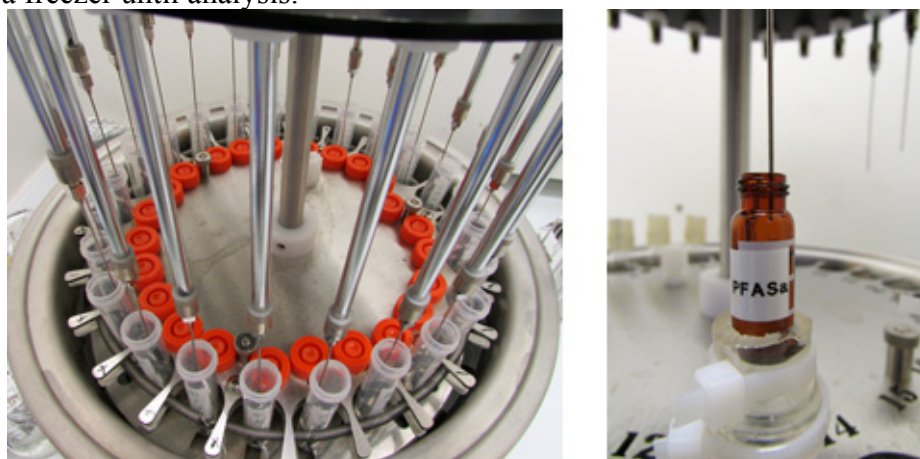


Figure 2. Concentration of eluted samples using N_2 stream. Left picture show 15 mL PP bottles before transfer to small brown glass vials (right).

Instrumental analysis

The extracted samples were analyzed according to method described by Ahrens et al. (2009) and calculated using the computer program *Agilent Technologies Masshunter Quantitative Analysis*. All integrations were checked manually. The instrument used was a high-performance liquid chromatography coupled with tandem mass spec-

trometry (HPLC-MS/MS), (Agilent Technologies 1200 series and Agilent Technologies 6040 Triple Quad LC/MS).

3.5.2. pH

Immediately following centrifugation of soil/solution mixture, pH was measured directly in the tubes at room temperature using a two-point calibrated PHM 93 reference pH meter from Radiometer Copenhagen.

3.5.3. Dissolved organic carbon

Half of the decanted liquid was filtered through 0.45 μm syringe filters (Acrodisc 32 mm syringe filters with Supor Membrane), and sent to ALS Scandinavia for analysis of dissolved organic carbon (DOC) for later use in Visual MINTEQ model (Appendix II).

3.5.4. Quality assurance/quality control (QA/QC)

Negative and positive control samples were utilized. PFASs levels in negative control samples (water) were all below detection limit. Losses of PFASs to container walls in positive control samples (water + PFASs) were corrected for by using reference standard (10 μL PFASs standard with 100 μL PFAS IS in methanol), which represents exact actual spiked concentration. The samples of the main experiment were prepared in duplicates. In total 36 samples were prepared, of which 32 contained soil.

Relative error between duplicates for compounds with shorter perfluorocarbon chain lengths ($\text{C}_3\text{-C}_8$ for PFCAs and C_4 for PFASs) were smaller (1.5-13%) than for longer perfluorocarbon chains ($\text{C}_9\text{-C}_{13}$ for PFCAs, $\text{C}_6\text{-C}_8$ for PFASs and FOSA (C_8)) where relative error ranged from 20 to 49% due to strong adsorption and therefore levels in liquid phase close to detection limit. Average relative error for whole dataset was 22%.

3.6. MODELLING OF NET CHARGE USING VISUAL MINTEQ

Visual MINTEQ is a freeware chemical equilibrium model originally built on USEPA's MINTEQA2 software, for natural waters, calculating for example acid-base equilibrium, metal speciation, solubility equilibrium and sorption (Gustafsson, 2013). In this study, Visual MINTEQ was used first to find suitable pH, and later to model net charge on the soil in the samples, which is dependent on pH, DOC, humic and fulvic acids and concentration of cations and anions.

Measured pH and DOC (Appendix II) and added Na-, Ca- and Al-nitrates (Table 4) together with concentrations of Mg, Fe, Mn, K, active humic acid (HA) and active fulvic acid (FA) from earlier analysis of the soil (Appendix I) were used as input. Input and output files can be found in Appendix I.

The overall net charge (Z^-) of the soil organic matter is given as mol L^{-1} . Ion concentrations was entered as fixed in the model, meaning that Visual MINTEQ calculated the concentrations of solid-phase organic complexes that were in equilibrium at the given dissolved concentrations. The net charge is calculated as the sum of the charge contributions from various different organic matter species in the solid phase. In the simple case of fulvic acid and with Al^{3+} and Ca^{2+} present in the soil solution, the value of Z^- is given by:

$$Z^- = RO^- - ROCa^+ - (RO)_2Al^+ \quad (1)$$

where RO^- is a dissociated functional group (carboxylate group), $ROCa^+$ is a complex involving one functional group and one Ca^{2+} ion, whereas $(RO)_2Al^+$ involves two functional groups and one Al^{3+} ion. The Z^- -value indicates the sum of negative charge on the organic matter (Löfgren et al., 2010).

3.7. DATA ANALYSIS

Since no extraction of PFASs in solid phase was done, the fraction sorbed to soil particles was approximated by the following formula:

$$c_s = (m_{std} - m_w) / m_{soil} \quad (2)$$

where c_s is the adsorbed PFAS on soil in $ng\ g^{-1}$. m_{std} is the mass of the spiked standard, m_w is the measured mass of the spiked compound in the aqueous phase of the sample and m_{soil} is the weight of the soil added. Where negative values on c_s were observed, the values were set to 0.

The particulate associated fraction φ (%) was calculated using the following formula:

$$\varphi = (m_s / m_{std}) \cdot 100 \quad (3)$$

where m_s is the approximated amount sorbed to the solid phase in ng.

The sediment–water distribution coefficient, K_d , was calculated using the following linear sorption model (Ahrens et al., 2011):

$$K_d = c_s / c_w \quad (4)$$

where c_w is the concentration of PFAS in the aqueous phase in $ng\ mL^{-1}$. Unit for K_d is $mL\ g^{-1}$.

The organic carbon normalised partition coefficient, K_{OC} , was calculated by the following formula (Ahrens et al., 2011):

$$K_{OC} = K_d / f_{OC} \quad (5)$$

where f_{OC} is the fraction organic carbon in $g\ C\ g^{-1}$ and the unit of K_{OC} is $mL\ g^{-1}$ (milli-litres per gram organic carbon).

4. RESULTS

4.1. BATCH SORPTION EXPERIMENT

4.1.1. PFCAs

Concentrations of the different PFCAs detected in the liquid phase vary, with concentrations close to initial concentration for shorter-chained compounds (PFBA, PFPeA, PFHxA), and with concentrations close to zero for longer-chained compounds (PFDA, PFUnDA, PFDODA, PFTeDA) (Figure 3). The measured initial concentration (reference standard) was used for the calculation of the sorption behavior of PFASs ranging from 450 ng L⁻¹ (PFTeDA) to 925 ng L⁻¹ (PFHxA). The deviation from the theoretical spiking concentration (i.e. 1248 ng L⁻¹) could be due to the age of the standard and loss due to sorption to the glass wall, but should not be a problem.

For PFCAs, a high variation of the individual PFCA concentrations was observed between the initial and final concentrations (after sorption experiments) in the liquid phase. The final concentration of PFHpA ranged between 500 and 790 ng L⁻¹, PFOA between 190 and 680 ng L⁻¹ and PFNA between 25 and 340 ng L⁻¹. Evident differences in the PFCAs concentrations between the different cations series could be observed for these compounds, with the series for NaNO₃ and 3 mM Ca(NO₃)₂ showing similar high concentrations, while Al(NO₃)₃ and 5 mM Ca(NO₃)₂ appear in lower concentrations in the liquid phase (Figure 3). Generally, concentrations for these compounds in the liquid phase increase with increasing pH. PFBA shows up in higher concentrations for some samples, in the liquid phase than in the reference samples (initial concentration), which is likely due to measurement uncertainties.

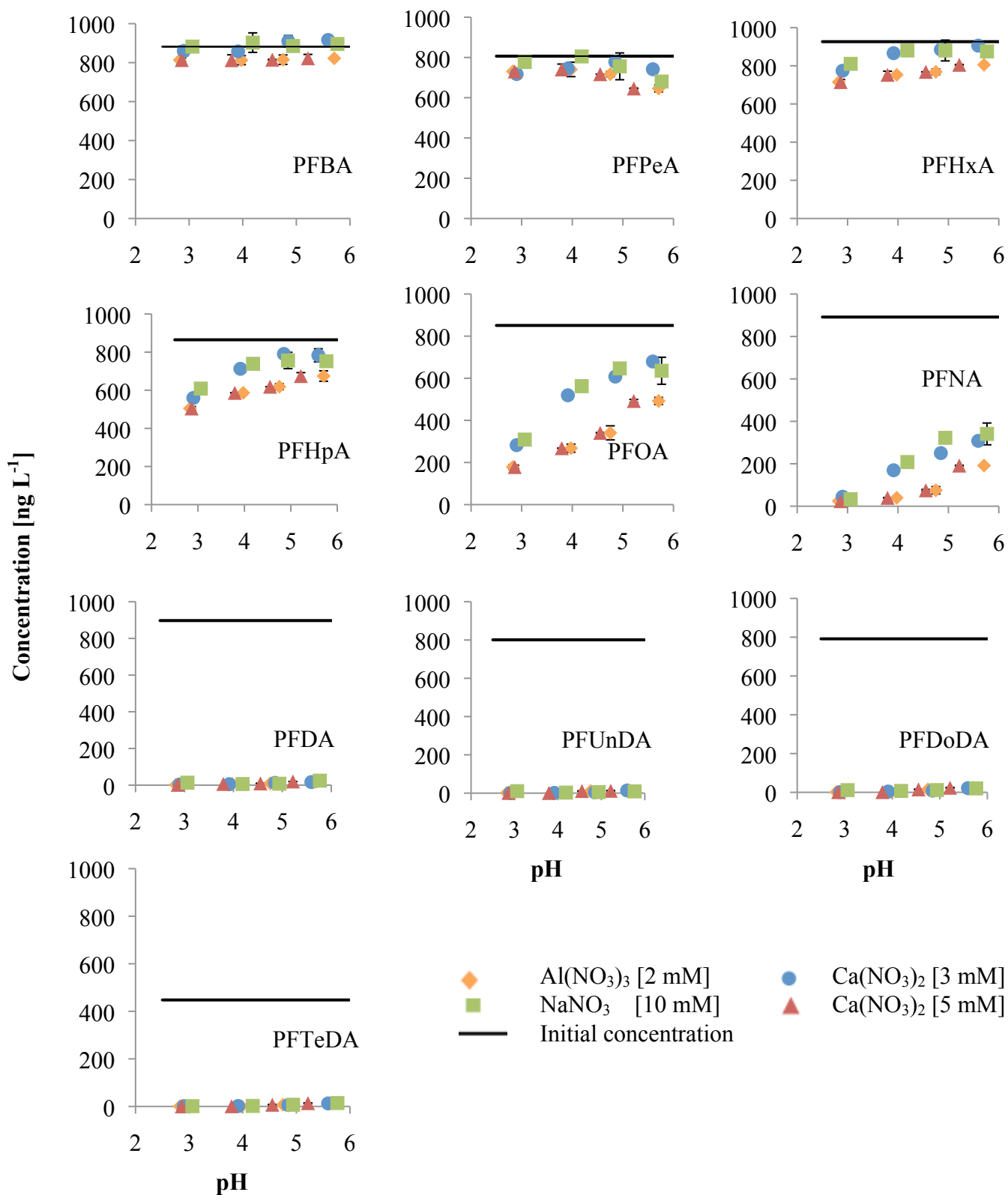


Figure 3. Concentration of PFCAs in solution (ng L^{-1}) as a function of pH after the sorption experiments using $\text{Al}(\text{NO}_3)_3$ [2 mM], NaNO_3 [10 mM], $\text{Ca}(\text{NO}_3)_2$ [3 mM] and $\text{Ca}(\text{NO}_3)_2$ [5 mM]. Black line represents measured initial concentrations, measured during the same run. Error bars represent standard deviations of duplicate samples.

4.1.2. PFSAs and FOSA

As shown in Figure 4, concentrations of the different PFSAs detected in the liquid phase also vary, as for the PFCAs, with concentrations close to initial concentration for the short-chained PFBS and with concentrations close to zero for the long-chained PFOS. For PFHxS, the concentrations span almost the whole range (17 to 560 ng L⁻¹), with the series for NaNO₃ and 3 mM Ca(NO₃)₂ showing similar high concentrations, while Al(NO₃)₃ and 5 mM Ca(NO₃)₂ appear in lower concentrations in the liquid phase. FOSA, with the same chain length as PFNA and PFOS, occur in concentrations close to zero, with initial concentration of 825 ng L⁻¹. PFBS show up in higher concentrations for some samples, in the liquid phase than in the reference (initial concentration), which is likely due to measurement uncertainties. Results from analysis are found in Appendix V.

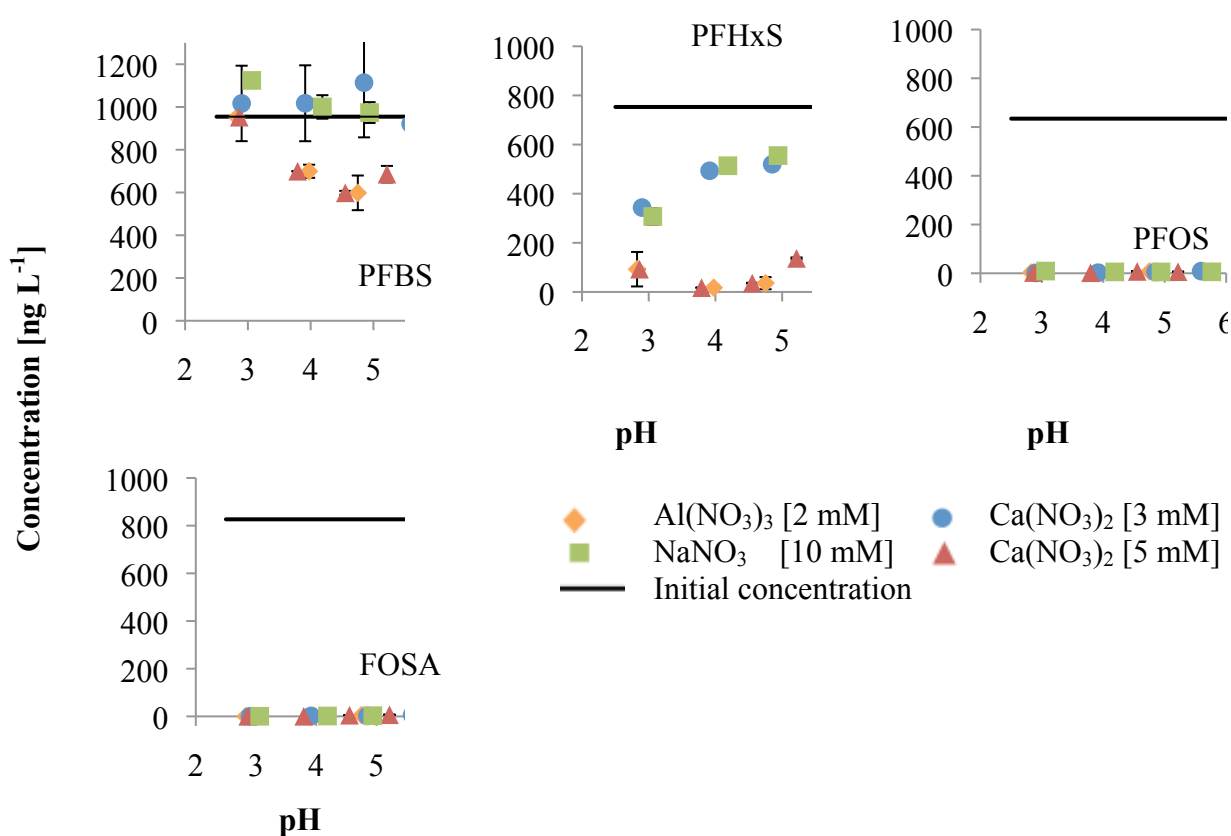


Figure 4. Concentration of PFSAs and FOSA in solution (ng L⁻¹) as a function of pH after the sorption experiments using Al(NO₃)₃ [2 mM], NaNO₃ [10 mM], Ca(NO₃)₂ [3 mM] and Ca(NO₃)₂ [5 mM]. Black line represents measured initial concentrations, measured during the same run. Error bars represent standard deviations of duplicate samples.

4.2. INFLUENCE OF CARBON CHAIN LENGTH AND FUNCTIONAL GROUPS ON SORPTION OF PFASs TO SOIL

The fraction of PFASs that adsorbs to particles can be described by the particulate associated fraction (% , Eq. 3). A clear trend between average increasing particulate associated fraction from all samples ($n = 31$) and perfluorocarbon chain length was observed for C₃-C₉ PFCAs (2.6-99%) and PFSAs (C₄-C₈, 8.2-99 %), (Figure 5). For the four PFCAs with the longest chains (i.e. PFDA, PFUnDA, PFDoDA, PFTeDA), the particulate associated fraction was close to 100%, and no clear trend visible among them. FOSA sorbed to nearly 100%.

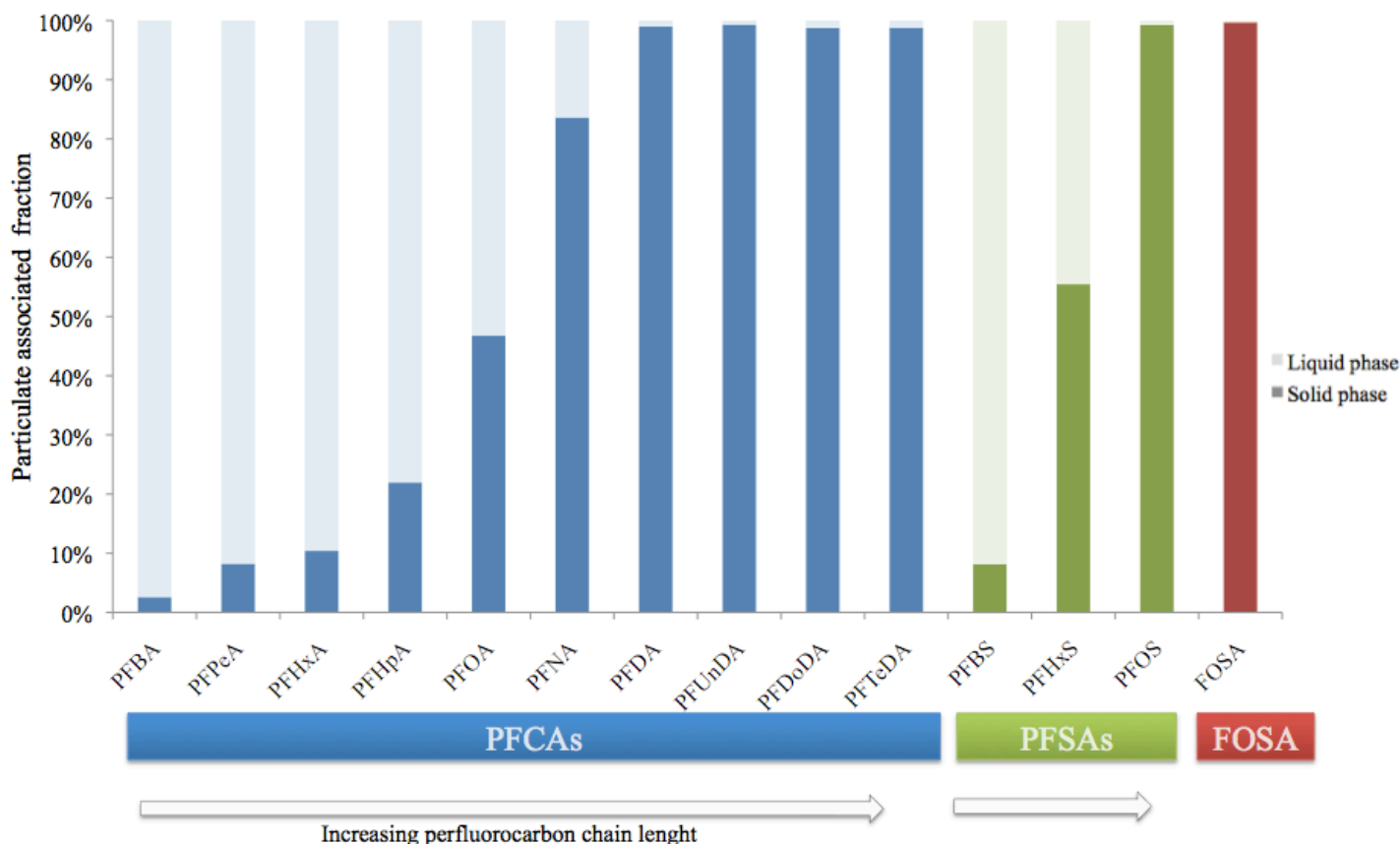


Figure 5. Particulate associated fraction of the different PFASs, grouped by PFCAs, PFSAs and FOSA, between solid (dark) and liquid (light) phase. Values represent the average for all samples (i.e. all tested pH-values and solution chemistries, $n=31$). The perfluorocarbon chain length increases to the right.

Another measure of sorption to soil is the K_d , which is normalised for solution volume and soil weight (Eq. 4), with a high K_d representing high sorption (i.e. large particulate associated fraction) and vice versa. Figure 6 shows the relationship between $\log K_d$ and the length of the fluorocarbon chain for PFCAs, PFSAs and FOSA, respectively. As with the associated particulate fraction, there was a clear trend between increased adsorption (i.e. higher $\log K_d$) and increasing perfluorocarbon chain length. The $\log K_d$ for PFSAs increased from 0.3 to 3.6 mL g⁻¹ for PFBS (C₄) to PFOS (C₈) ($R^2=0.98$). For PFCAs, the $\log K_d$ increased linearly from -0.1 (C₃) to 3.8 ml g⁻¹ (C₁₀) ($R^2=0.93$), and then tapered off.

The PFSAs (sulfonate functional group) adsorbed more strongly (slope 0.84) than the PFCAs (carboxylic functional group, slope 0.60) for the same number of carbon atoms in the chain. The FOSA adsorbed the strongest, with $\log K_d$ value of 4.2 ml g^{-1} . Similar trends for K_{OC} (Eq 5) were observed (Table 5). Average K_d and K_{OC} for the different cation-series are found in Appendix VI along with all K_d -values in Appendix VII.

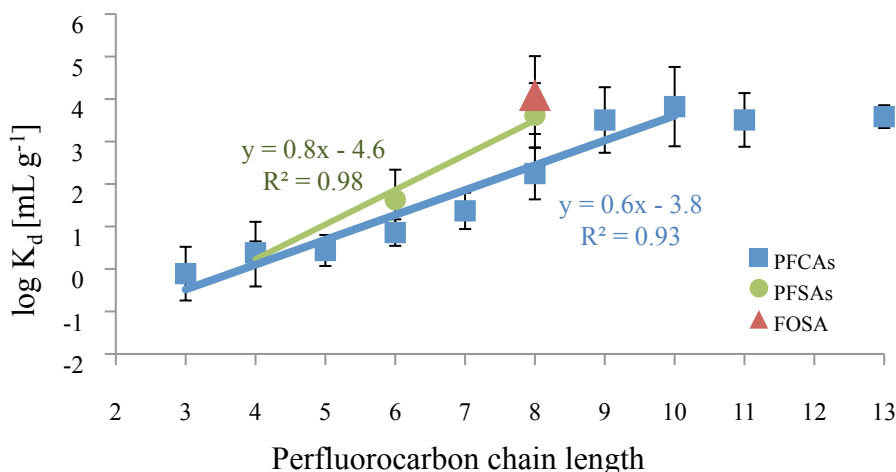


Figure 6. Average log partitioning coefficient (K_d) as a function of perfluorocarbon chain length for PFCAs, PFSAs and FOSA. Lines represent linear regressions for PFSAs (i.e. PFBS (C_4) to PFOS (C_8)) and PFCAs (i.e. PFBA (C_3) to PFUnDA (C_{10})). Error bars represent standard deviation of all samples for each compound (i.e. all tested pH-values and solution chemistries, $n =$ see Table 5).

Table 5. Average Log K_d and log K_{OC} for all samples, with standard deviation. K_d calculated by Eq. 4 and K_{OC} calculated by Eq. 5.

[mL g^{-1}]	Log K_d	Log K_{OC}	(n)
Compound	\pm SD	\pm SD	
PFBA	-0.1 \pm 0.6	0.2 \pm 0.6	(19)
PFPeA	0.4 \pm 0.3	0.7 \pm 0.3	(30)
PFHxA	0.4 \pm 0.4	0.8 \pm 0.4	(31)
PFHpA	0.9 \pm 0.3	1.2 \pm 0.3	(31)
PFOA	1.4 \pm 0.4	1.8 \pm 0.4	(31)
PFNA	2.2 \pm 0.5	2.7 \pm 0.5	(31)
PFDA	3.5 \pm 0.4	4.0 \pm 0.4	(31)
PFUnDA	3.8 \pm 0.6	4.3 \pm 0.6	(31)
PFDoDA	3.5 \pm 0.6	4.0 \pm 0.6	(31)
PFTeDA	3.6 \pm 0.7	4.0 \pm 0.7	(31)
PFBS	0.3 \pm 0.8	0.7 \pm 0.8	(18)
PFHxS	1.6 \pm 0.7	2.0 \pm 0.7	(31)
PFOS	3.6 \pm 0.8	4.1 \pm 0.4	(31)
FOSA	4.1 \pm 0.9	4.6 \pm 0.5	(31)

4.3. INFLUENCE OF CATIONS, PH AND NET NEGATIVE CHARGE ON SORPTION OF PFASs TO SOIL

The net charge of the soil surface is dependent on the pH. Figure 7 shows how the modelled net negative charge changed with pH for $\text{Al}(\text{NO}_3)_3$ [2 mM], NaNO_3 [10 mM], $\text{Ca}(\text{NO}_3)_2$ [3 mM] and $\text{Ca}(\text{NO}_3)_2$ [5 mM]. For low pH (~3) the difference between the NaNO_3 and the two $\text{Ca}(\text{NO}_3)_2$ -series were small ($\pm 9\%$), with $\text{Al}(\text{NO}_3)_3$ being lower. For NaNO_3 , the relation was linear for the interval. The two $\text{Ca}(\text{NO}_3)_2$ -series compared with $\text{Al}(\text{NO}_3)_3$ showed inverse correlations, with $\text{Ca}(\text{NO}_3)_2$ increasing rapidly and then taping off, whereas $\text{Al}(\text{NO}_3)_3$ started off slow and then increased rapidly presenting a higher value for pH~6.

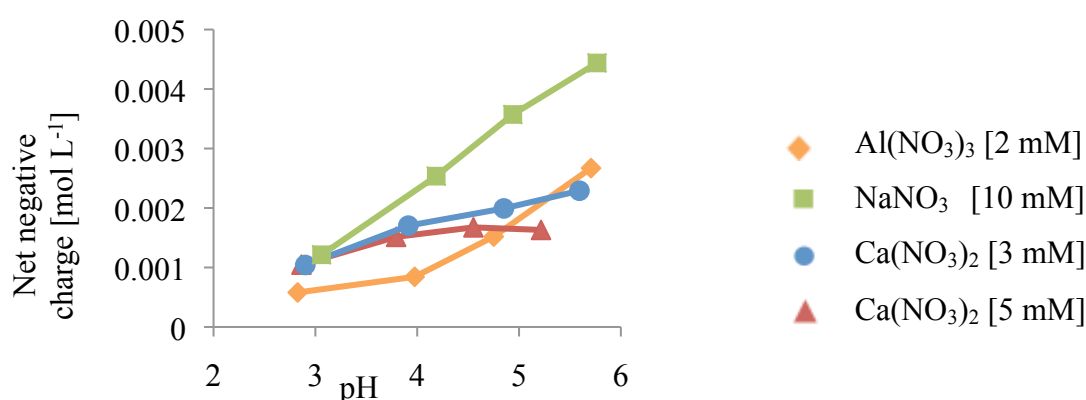


Figure 7. Modelled net charge as a function of pH (measured).

4.3.1. Influence of cations and pH on sorption of PFASs to soil

PFCA_s

The calculated $\log K_d$ values were plotted against pH for PFCAs (Figure 8), and PFSA_s and FOSA (Figure 9). For most PFCAs, there was a general trend of decreasing sorption with increasing pH, with the exception of PFBA (C_3) that showed no correlation and PFPeA (C_4) but instead showed increasing $\log K_d$ with increasing pH for $\text{Al}(\text{NO}_3)_3$ (0.5–0.9 mL g^{-1}), NaNO_3 (0.0–0.7 mL g^{-1}) and $\text{Ca}(\text{NO}_3)_2$ with the higher concentration (5 mM) (0.2–0.5 mL g^{-1}). PFHxA (C_5 , $\log K_d$ range -0.2–0.9 mL g^{-1}), PFHpA (C_6 , $\log K_d$ range 0.4–1.3 mL g^{-1}), PFOA (C_7 , $\log K_d$ range 0.9–2.1 mL g^{-1}) and PFNA (C_8 , $\log K_d$ range 1.7–3.0 mL g^{-1}) showed decreasing sorption with increasing pH, and also distinct difference among the cation-series. The $\text{Al}(\text{NO}_3)_3$ -series presented the highest $\log K_d$ -values consistently over the pH interval for these compounds, followed by $\text{Ca}(\text{NO}_3)_2$ (5 mM). $\text{Ca}(\text{NO}_3)_2$ (3 mM) and NaNO_3 appeared with similar range of values. For lower pH, the differences between the different series were small, with very little difference between the sodium- and the two calcium-series. As pH increased, the difference was more pronounced. For PFDA (C_9 , $\log K_d$ range 3.1–4.7 mL g^{-1}), PFUnDA (C_{10} , $\log K_d$ range 3.3–5.1 mL g^{-1}), PFDoDA (C_{11} , $\log K_d$ range 3.1–4.5 mL g^{-1}) and PFTeDA (C_{13} , $\log K_d$ range 3.0–4.7 mL g^{-1}), the $\log K_d$ were in the same range and there was less or no influence by the different cations.

PFSAs and FOSA

PFBS (C_4 , K_d range 1.2–1.2 mL g⁻¹), PFHxS (C_6 , K_d range 1.0–3.1 mL g⁻¹) and PFOS (C_8 , K_d range 3.5–4.1 mL g⁻¹) (Figure 9), showed no evident trend with pH. There was however a large difference between the cation-series, for PFHxS, with Al(NO₃)₃ (2.4–3.1 mL g⁻¹) having two to three times higher log K_d than Ca(NO₃)₂ (5 mM), Ca(NO₃)₂ (3 mM) and NaNO₃, which all appeared within the same range of values (1.0–1.6 mL g⁻¹). FOSA (C_8 , K_d range 3.6–5.1 mL g⁻¹), however, showed a decreasing trend with increasing pH, similar to the one of the long-chained PFCAs (C₁₀-C₁₃, Figure 8).

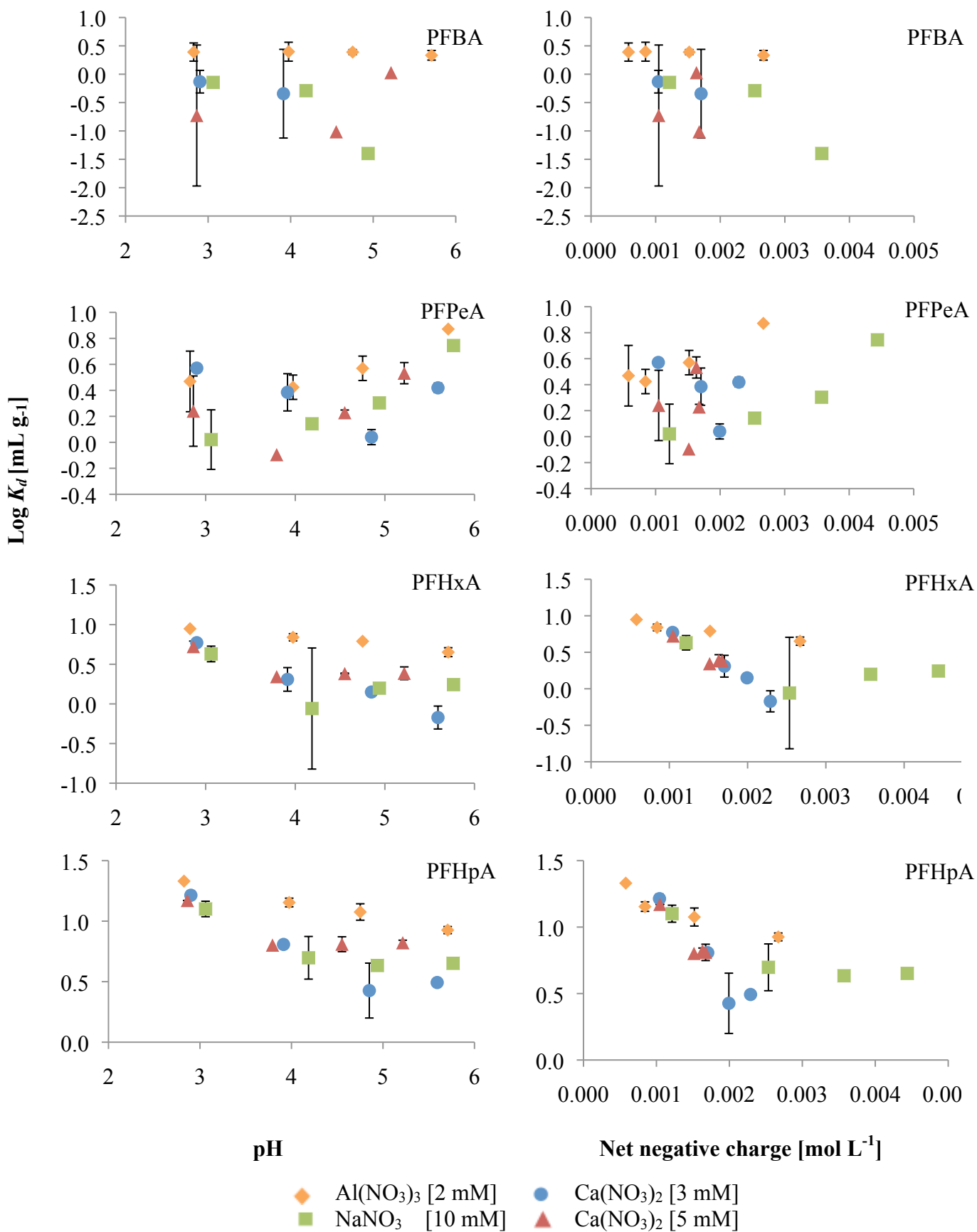
4.3.2. Influence of cations and net negative charge on sorption of PFSAs to soil

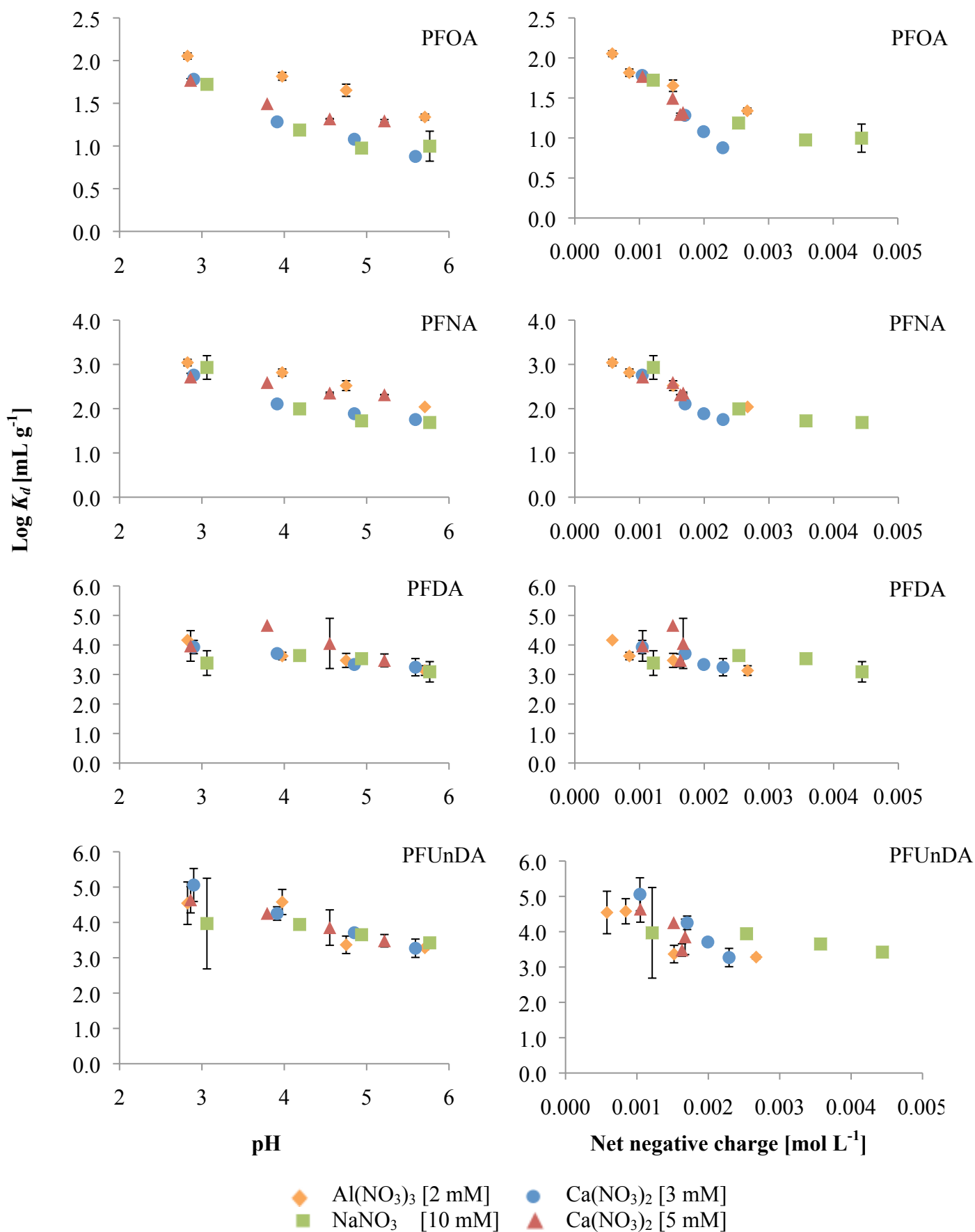
PFCAs

PFBA and PFPeA showed no clear correlations with net negative charge, however for fluorocarbon chains C₅ and longer (PFHxA–PFTeDA) there were decreasing trends with increasing pH, especially linear for net negative charge 0–0.025 mol L⁻¹. The differences between the different cation-series were not prominent, except for the NaNO₃ that showed higher values of net negative charge, in agreement with Figure 7.

PFSAs and FOSA

PFBS, PFHxS and PFOS (Figure 9) showed no evident trend with net negative charge. But as for pH, there was a large difference between the cation-series, for PFHxS, with Al(NO₃)₃ appearing above Ca(NO₃)₂ (5 mM), Ca(NO₃)₂ (3 mM) and NaNO₃ in the graph. FOSA however, showed a similar net negative charge trend as the long-chained PFCAs (C₁₀-C₁₃, Figure 8).





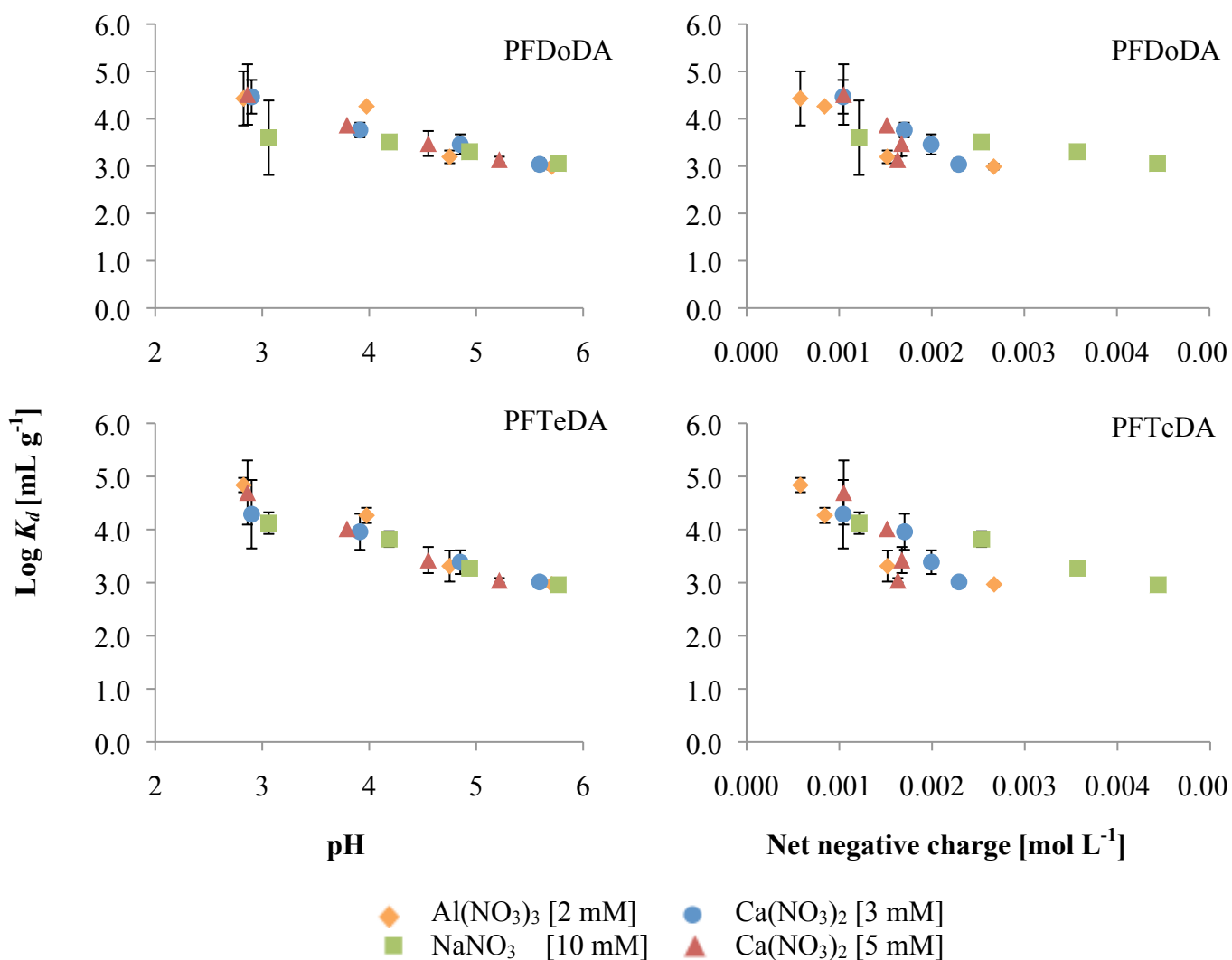


Figure 8. Logarithm distribution coefficient (K_d) as a function of pH (left) and net negative charge (right) for PFCAs. Error bars represents standard deviation between duplicate samples.

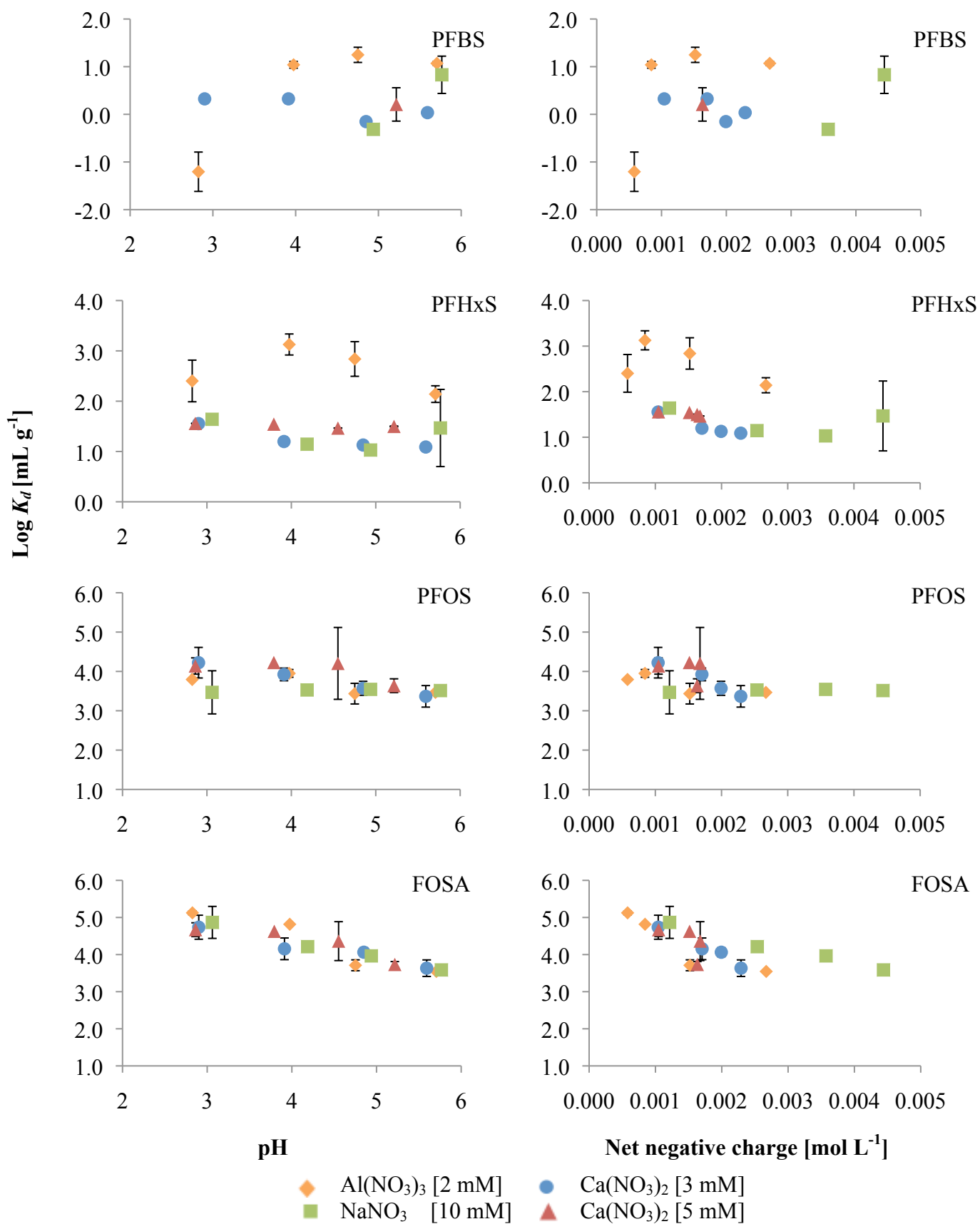


Figure 9. Logarithm distribution coefficient (K_d) as a function of pH (left) and net negative charge (right) for PFSA and FOSA. Error bars represents standard deviation between duplicate samples.

5. DISCUSSION

5.1. BATCH SORPTION EXPERIMENTS

Concentrations of individual PFASs detected in the liquid phase varied (Figure 8 and Figure 9), with concentrations close to the initial concentration for shorter-chained compounds (i.e. low sorption to soil particles) and with concentrations close to zero for longer-chained compounds. This indicates that the longer the perfluorocarbon chain length, and the stronger the influence of the functional group, the more likely that the compounds will adsorb to soil particles. PFBA and PFBS showed for some samples slightly higher concentrations in the liquid phase in the soiled samples than for the reference due to analytical uncertainties, thus the log K_d and log K_{OC} for PFBA should be handled with care (Table 6). PFDA, PFUnDA, PFDoDA, PFTeDA, PFOS and FOSA were found in levels close to the detection limit and hence these data are more uncertain and with higher relative errors than the other compounds.

5.2. INFLUENCE OF CARBON CHAIN LENGTH AND FUNCTIONAL GROUPS ON SORPTION OF PFASs TO SOIL

Sorption of PFASs to organic matter is a balance between two counteracting forces: firstly attraction forces between the hydrophobic ‘tail’ (i.e. perfluorocarbon chain) of PFASs and hydrophobic parts of soil organic matter and secondly repulsion forces between the negatively charged ‘head’ (functional group) of the PFASs molecules and the negatively charged carboxylic groups of soil organic matter.

In accordance with earlier research, the adsorption of PFASs in this study was strongly correlated with perfluorocarbon chain length (Ahrens et al., 2010; Du et al., 2014; Higgins and Luthy, 2006; Labadie and Chevreuril, 2011), where the longer the perfluorocarbon chain (i.e. more hydrophobic) the stronger the adsorption to particles was (Figure 5 and Figure 6). This can be explained with the increase in hydrophobic attraction forces between PFAS molecules and organic matter with increased carbon chain length of the PFAS molecule. The log K_d and perfluorocarbon chain length displayed a positively linear relationship for all PFASs and for C₃ to C₁₀ for PFCAs (Figure 6).

As reported in previous studies (Ahrens et al., 2010; Higgins and Luthy, 2006), this study also found that the PFASs sorbed stronger to particles than PFCAs. This indicates that the functional group has an impact on sorption, due to the electrostatic negatively charged functional group of the PFAS molecule functional head (Du et al., 2014).

The calculated log K_d (Eq. 4) and log K_{OC} (Eq. 5) were compared to previous studies (Table 6). In general, the log K_d , and log K_{OC} were in the same range as previous studies and showed an increasing trend with increased perfluorocarbon chain length, which is also consistent with previous studies (Ahrens et al., 2011, 2010; Higgins and Luthy, 2006; Labadie and Chevreuril, 2011). The differences between values from this study and others could be due to the very different carbon contents (45% for this study compared to 0-10.6%), and the possibility of relationship between carbon content and sorption not behaving linearly.

Table 6. Log K_d and log K_{OC} (\pm standard deviation (SD)) in this study in comparison with log K_{oc} from other studies (Ahrens et al., 2011, 2010; Higgins and Luthy, 2006; Labadie and Chevreuil, 2011).

	Log K_d \pm SD	Log K_{OC} \pm SD	Log K_{OC} \pm SD	Log K_{OC} \pm SD	Log K_{OC} \pm SD	Log K_{OC} \pm SD
[mL g ⁻¹]	This study ^a	This study ^a	(n) Higgins and Luthy, 2006 ^b	(n) Ahrens et al., 2011 ^c	(n) Ahrens et al., 2010 ^d	(n) Labadie and Chevreuil, 2011 ^e
PFBA	-0.1 \pm 0.6	0.2 \pm 0.6	(19)			
PFPeA	0.4 \pm 0.3	0.7 \pm 0.3	(30)			
PFHxA	0.4 \pm 0.4	0.8 \pm 0.4	(31)			2.1 \pm 0.2 (3)
PFHpA	0.9 \pm 0.3	1.2 \pm 0.3	(31)		2.9 \pm 0.0 (6)	2.1 \pm 0.2 (3)
PFOA	1.4 \pm 0.4	1.8 \pm 0.4	(31)	2.1 \pm - (2)	2.4 \pm 0.2 (9)	3.5 \pm 0.1 (6)
PFNA	2.2 \pm 0.5	2.7 \pm 0.5	(31)	2.4 \pm 0.1 (3)		4.0 \pm 0.1 (6)
PFDA	3.5 \pm 0.4	4.0 \pm 0.4	(31)	2.8 \pm 0.1 (5)		4.6 \pm 0.1 (6)
PFUnDA	3.8 \pm 0.6	4.3 \pm 0.6	(31)	3.3 \pm 0.1 (5)		5.1 \pm 0.1 (6)
PFDoDA	3.5 \pm 0.6	4.0 \pm 0.6	(31)			4.7 \pm 0.1 (3)
PFTeDA	3.6 \pm 0.7	4.0 \pm 0.7	(31)			5.6 \pm 0.2 (3)
PFBS	0.3 \pm 0.8	0.7 \pm 0.8	(18)			
PFHxS	1.6 \pm 0.7	2.0 \pm 0.7	(31)			3.7 \pm 0.3 (6)
PFOS	3.6 \pm 0.4	4.1 \pm 0.4	(31)	2.6 \pm 0.1 (4)	3.5 \pm 0.9 (18)	4.8 \pm 0.1 (6)
FOSA	2.7 \pm 0.5	4.6 \pm 0.5	(31)		4.2 \pm 1.0 (22)	4.5 \pm 0.1 (6)

^a Organic soil with 45 % carbon content

^b Organic carbon content in sediment ranging from 0-10%.

^c Organic carbon content in sediment ranging from 0-1.6 %

^d Organic carbon content in sediment ranging from 1.5-10.6 %.

^e Organic carbon content in sediment 4.8%

n = number of samples included in the calculation

5.3. INFLUENCE OF CATIONS, PH AND NET NEGATIVE CHARGE ON SORPTION OF PFAS TO SOIL

5.3.1. Influence of pH

For most PFCAs, (C₅-C₁₃) and FOSA there was a general trend of decreasing log K_d (i.e. sorption), with increasing pH, with the exception of PFBA that shows no correlation and PFPeA that rather show increasing log K_d with increasing pH (Figure 8). This is in accordance with previous studies which showed also a negative correlation between the log K_d and increasing pH as also other studies have found (Chen et al., 2009; Du et al., 2014; Higgins and Luthy, 2006; Tang et al., 2010; Wang et al., 2012). In contrast, the PFSA (Figure 9), showed no clear correlation between log K_d and pH.

Due to the very low pK_a of the PFASs (<0.14 for all compounds except FOSA, Table 1), they are predominately present in their ionized form in the aqueous environment (Ahrens et al., 2012). Thus, at the pH range of 3 to 6, as investigated in this study, the PFASs will be present in their ionized form. However, a change of the pH will change the protonation/deprotonation of the sorbate, as with the increase of pH, adsorbent surfaces tend to become more negatively charged (Figure 7) leading to stronger electrostatic repulsion, and hence lower sorption (Chen et al., 2009; Higgins and Luthy, 2006). This effect was observed as a trend regardless of perfluorocarbon chain length for the PFCAs and FOSA, although results for C₃ and C₄ were uncertain.

5.3.2. Influence of cations

For short and intermediate perfluorocarbon chain length PFCAs (C₅-C₈) and PFHxS among the PFASs, cation concentrations had an effect on sorption. The difference between the different cations were smaller at lower pH, with very little difference between the NaNO₃- and the two Ca(NO₃)₂-series (Figure 8 and Figure 9). As pH increased, the differences between the series increased with Al(NO₃)₃ showing the highest sorption followed by Ca(NO₃)₂ (5 mM). The adsorption was higher when more calcium ions were present (i.e. higher log *K_d* for 5 mM Ca(NO₃)₂ than for 3mM Ca(NO₃)₂), which also was found also earlier studies (Chen et al., 2009; Higgins and Luthy, 2006; You et al., 2010). There was no clear difference between 3 mM Ca(NO₃)₂ and NaNO₃. For PFDA, PFUnDA, PFDoDA and PFTeDA (C₉-C₁₃), the data-points for all cations (i.e. Ca(NO₃)₂ (5 and 3 mM), Al(NO₃)₃ and NaNO₃) were close together, with no clear trends, indicating that influence by the different cations is less important for sorption at longer perfluorocarbon chains.

According to Higgins and Luthy (2006), the effect of Ca²⁺ on sorption is due to a reduction in the charge present (and repulsive forces) on the organic matter, and partially neutralizes the negative surface charge by interactions between the functional groups (carboxylic groups) present in the organic matter, resulting in an increase in the sorption between the surface of the organic matter and the PFASs. Higgins and Luthy (2006) observed that this neutralization effect is stronger when the Ca²⁺-concentration increases, which could be confirmed in this study. Trivalent ions, such as Al³⁺ have a higher capacity to neutralize surface charge than divalent ions (such as Ca²⁺), which is why the sorption was stronger with Al(NO₃)₃ present, even though the Al(NO₃)₃-concentration was lower (2 mM) than for Ca(NO₃)₂ (3 and 5 mM respectively). NaNO₃ (Na⁺, univalent) had the least influence on sorption, which was also reported in other studies (Higgins and Luthy, 2006).

5.3.3. Influence of net negative charge

The net charge was calculated with the geochemical model Visual MINTEQ, which takes into many parameters when calculating net charge on the soil surface. One of the aims of this study was to investigate whether modelled net charge correlates better with sorption of PFASs than cation composition and pH alone.

For PFCAs (C₅-C₁₃) and FOSA, log *K_d* (Figure 8) showed good a correlation with net negative charge, with low net negative (i.e. neutralized soil surface) resulting in the highest log *K_d*-values. For Al(NO₃)₃, the net negative charge was generally the lowest, followed by Ca(NO₃)₂ (5 mM), Ca(NO₃)₂ (3 mM) and NaNO₃. For PFBA, PFPeA, PFBS, PFHxS and PFOS, net negative charge does not explain the high log *K_d* for Al(NO₃)₃. Log *K_d* for PFOS remains relatively constant with net charge.

5.3.4. Comparison between pH and net negative charge

When comparing the correlation of *K_d* vs pH and *K_d* vs net negative charge (Figure 8 and Figure 9), the net negative charge showed less spreading of the data for all cations for PFHxA, PFHpA, PFOA and PFNA than for pH. This indicates a better correlation, i.e. that net negative charge is a better predictor for the sorption for these compounds than pH is. For PFDA and longer-chained PFCAs (C₉-C₁₃), the difference between pH and net negative charge was less pronounced, with pH showing slightly better linearity. For PFBA and PFPeA, no correlation was found.

For PFHxS, $\log K_d$ for $\text{Al}(\text{NO}_3)_3$ was much higher than the other cations, which can be neither explained by pH nor net negative charge. It is possible that this is due to complex formations, however the results of this study cannot confirm this. $\log K_d$ for PFOS showed no correlation with either net negative charge or pH, but were rather constant over the interval. FOSA correlates equally well with both net negative charge and pH.

Overall, the net negative charge is for some PFASs a better predictor for sorption of PFASs to soil. This can be explained by the fact that the charge present on the soil surface is the main factor that affects the sorption of PFASs to soil. Thus, net charge is potentially a better predictor of sorption to soil than solution pH alone (which is based only on the H^+ -concentration).

5.4. FUTURE PERSPECTIVES

This study shows that net charge, pH, cation concentrations are important parameters influencing the sorption of PFASs to soil. More studies are needed for cations with different valence and of different concentrations. Furthermore, this study was limited to soil rich in organic carbon, more studies are needed to compare the results from this study with mineral soil and sediments. Eventually, these results could be used to implement a feature of PFASs sorption to soil into a geochemical model such as Visual MINTEQ, to better predict the fate of PFASs in the environment.

6. CONCLUSION

The aims of this study was to investigate the effects of pH, cation composition, functional group and perfluorocarbon chain length on sorption of PFASs to soil particles, by batch sorption experiment in laboratory scale. The laboratory-scale experiments were combined with modelling of the net charge to evaluate net charge is a good predictor for sorption of PFASs to soil particles.

The adsorption of PFASs was strongly correlated with perfluorocarbon chain length, showing a stronger adsorption to particles with increasing perfluorocarbon chain length (i.e. more hydrophobic). The relation between $\log K_d$ and perfluorocarbon chain length was linear for all PFASs and C_3 to C_{10} PFCAs (Figure 6). The FASAs (sulfonate functional group) sorbed stronger to soil particles than the PFCAs (carboxylic functional group), whereas FOSA (sulfonamide functional group) sorbed the strongest.

For most PFCAs, (C_5 - C_{13}) there was a trend of decreasing $\log K_d$ (i.e. sorption) with increasing pH. A change of pH will change the protonation/deprotonation of the soil surface, thus with increase of pH, adsorbent surfaces tend to become more negatively charged. This stronger electrostatic repulsion resulted in lower sorption for high pH. This effect was observed as a trend regardless of perfluorocarbon chain length for the PFCAs and FOSA.

For short and intermediate perfluorocarbon chain length PFCAs (C_5 - C_8) and PFHxS among the PFASs, cation concentrations had a clear effect on sorption. The adsorption was higher when more calcium ions were present (i.e. higher $\log K_d$ for 5 mM $\text{Ca}(\text{NO}_3)_2$ than for 3mM $\text{Ca}(\text{NO}_3)_2$), and $\text{Al}(\text{NO}_3)_3$ consistently showed the highest $\log K_d$ for these compounds. NaNO_3 had the least influence on sorption. This effect is due

to the positive cations which partially neutralizes the negative surface charge by interactions between the functional groups (carboxylic groups) present in the organic matter, resulting in an increase in the sorption between the surface of the organic matter and the PFASs. Trivalent ions, such as Al^{3+} has a higher capacity to neutralize surface charge than divalent ions (such as Ca^{2+}), which is why the sorption was stronger with $\text{Al}(\text{NO}_3)_3$ present.

The net charge modelled with Visual MINTEQ takes into account many parameters (including pH) that affect the surface charge and sorption of PFASs to soil particles. When comparing K_d for the different PFASs with pH and net negative charge, net charge was a better predictor of sorption of PFASs to soil particles than solution pH alone.

7. REFERENCES

- Ahrens, L., Harner, T., Shoeib, M., Lane, D.A., Murphy, J.G., 2012. Improved Characterization of Gas–Particle Partitioning for Per- and Polyfluoroalkyl Substances in the Atmosphere Using Annular Diffusion Denuder Samplers. *Environ. Sci. Technol.* 46, 7199–7206.
- Ahrens, L., Taniyasu, S., Yeung, L.W.Y., Yamashita, N., Lam, P.K.S., Ebinghaus, R., 2010. Distribution of polyfluoroalkyl compounds in water, suspended particulate matter and sediment from Tokyo Bay, Japan. *Chemosphere* 79, 266–272.
- Ahrens, L., Yamashita, N., Yeung, L.W.Y., Taniyasu, S., Horii, Y., Lam, P.K.S., Ebinghaus, R., 2009. Partitioning Behavior of Per- and Polyfluoroalkyl Compounds between Pore Water and Sediment in Two Sediment Cores from Tokyo Bay, Japan. *Environ. Sci. Technol.* 43, 6969–6975.
- Ahrens, L., Yeung, L.W.Y., Taniyasu, S., Lam, P.K.S., Yamashita, N., 2011. Partitioning of perfluorooctanoate (PFOA), perfluorooctane sulfonate (PFOS) and perfluorooctane sulfonamide (PFOSA) between water and sediment. *Chemosphere* 85, 731–737.
- Borg, D., Håkansson, H., 2012. Environmental and Health Risk Assessment of Perfluoroalkylated and Polyfluoroalkylated Substances (PFASs) in Sweden (No. Report 6513). Naturvårdsverket.
- Buck, R.C., Franklin, J., Berger, U., Conder, J.M., Cousins, I.T., de Voogt, P., Jensen, A.A., Kannan, K., Mabury, S.A., van Leeuwen, S.P., 2011. Perfluoroalkyl and polyfluoroalkyl substances in the environment: Terminology, classification, and origins. *Integr. Environ. Assess. Manag.* 7, 513–541.
- Chen, H., Chen, S., Quan, X., Zhao, Y., Zhao, H., 2009. Sorption of perfluorooctane sulfonate (PFOS) on oil and oil-derived black carbon: Influence of solution pH and [Ca²⁺]. *Chemosphere* 77, 1406–1411.
- Du, Z., Deng, S., Bei, Y., Huang, Q., Wang, B., Huang, J., Yu, G., 2014. Adsorption behavior and mechanism of perfluorinated compounds on various adsorbents—A review. *J. Hazard. Mater.* 274, 443–454.
- Giesy, J.P., Kannan, K., 2002. Perfluorochemical surfactants in the environment. *Environ. Sci. Technol.* 36, 146A–152A.
- Glynn, A., Aune, M., Darnerud, P.O., Cnattingius, S., Bjerselius, R., Becker, W., Lignell, S., 2007. Determinants of serum concentrations of organochlorine compounds in Swedish pregnant women: a cross-sectional study. *Environ. Health* 6, 2.
- Glynn, A., Berger, U., Bignert, A., Ullah, S., Aune, M., Lignell, S., Darnerud, P.O., 2012. Perfluorinated Alkyl Acids in Blood Serum from Primiparous Women in Sweden: Serial Sampling during Pregnancy and Nursing, And Temporal Trends 1996–2010. *Environ. Sci. Technol.* 46, 9071–9079.
- Glynn, A., Cantillana, T., Bjeremo, H., 2013. Riskvärdering av perfluorerande alkylsyror i livsmedel och dricksvatten (No. Rapport 11 - 2013). Livsmedelsverket.
- Gustafsson, J.P., 2013. Visual MINTEQ – a free equilibrium speciation model [WWW Document]. KTH Vis. MINTEQ. URL <http://vminTEQ.lwr.kth.se/> (accessed 5.7.15).
- Gustafsson, J.P., Persson, I., Oromieh, A.G., van Schaik, J.W.J., Sjöstedt, C., Kleja, D.B., 2014a. Chromium(III) Complexation to Natural Organic Matter: Mechanisms and Modeling. *Environ. Sci. Technol.* 48, 1753–1761.

- Gustafsson, J.P., Persson, I., Oromieh, A.G., van Schaik, J.W.J., Sjöstedt, C., Kleja, D.B., 2014b. Chromium(III) Complexation to Natural Organic Matter: Mechanisms and Modeling. Supporting information.
- Hansen, K.J., Clemen, L.A., Ellefson, M.E., Johnson, H.O., 2001. Compound-Specific, Quantitative Characterization of Organic Fluorochemicals in Biological Matrices. *Environ. Sci. Technol.* 35, 766–770.
- Hedenberg, G., 2014. Miljögifter i vatten – faroanalys behövs. *Sven. Vatten*.
- Higgins, C.P., Luthy, R.G., 2006. Sorption of Perfluorinated Surfactants on Sediments. *Environ. Sci. Technol.* 40, 7251–7256.
- Johnson, R.L., Anschutz, A.J., Smolen, J.M., Simcik, M.F., Penn, R.L., 2007. The Adsorption of Perfluorooctane Sulfonate onto Sand, Clay, and Iron Oxide Surfaces. *J. Chem. Eng. Data* 52, 1165–1170.
- Kannan, K., Corsolini, S., Falandysz, J., Fillmann, G., Kumar, K.S., Loganathan, B.G., Mohd, M.A., Olivero, J., Wouwe, N.V., Yang, J.H., others, 2004. Perfluorooctanesulfonate and related fluorochemicals in human blood from several countries. *Environ. Sci. Technol.* 38, 4489–4495.
- Kärman, A., van Bavel, B., Järnberg, U., Hardell, L., Lindström, G., 2006. Perfluorinated chemicals in relation to other persistent organic pollutants in human blood. *Chemosphere* 64, 1582–1591.
- Kim, M., Li, L.Y., Grace, J.R., Yue, C., 2015. Selecting reliable physicochemical properties of perfluoroalkyl and polyfluoroalkyl substances (PFASs) based on molecular descriptors. *Environ. Pollut.* 196, 462–472.
- Kudo, N., Bandai, N., Suzuki, E., Katakura, M., 2000. Induction by perfluorinated fatty acids with different carbon chain length of peroxisomal beta-oxidation in the liver of rats. *Chem. Biol. Interact.* 124, 119–132.
- Labadie, P., Chevreuil, M., 2011. Partitioning behaviour of perfluorinated alkyl contaminants between water, sediment and fish in the Orge River (nearby Paris, France). *Environ. Pollut.* 159, 391–397.
- Livsmedelsverket, 2015. Riskhantering - PFAA i dricksvatten [WWW Document]. URL <http://www.livsmedelsverket.se/livsmedel-och-innehall/oonskade-amnen/miljogifter/PFAS-poly-och-perfluorerade-alkylsubstanser/riskhantering-pfaa-i-dricksvatten/> (accessed 4.25.15).
- Löfgren, S., Gustafsson, J.P., Bringmark, L., 2010. Decreasing DOC trends in soil solution along the hillslopes at two IM sites in southern Sweden — Geochemical modeling of organic matter solubility during acidification recovery. *Sci. Total Environ.* 409, 201–210.
- Martin, J.W., Mabury, S.A., Solomon, K.R., Muir, D.C., 2003. Bioconcentration and tissue distribution of perfluorinated acids in rainbow trout (*Oncorhynchus mykiss*). *Environ. Toxicol. Chem.* 22, 196–204.
- Milinovic, J., Lacorte, S., Vidal, M., Rigol, A., 2015. Sorption behaviour of perfluoroalkyl substances in soils. *Sci. Total Environ.* 511, 63–71.
- Moody, C.A., Hebert, G.N., Strauss, S.H., Field, J.A., 2003. Occurrence and persistence of perfluorooctanesulfonate and other perfluorinated surfactants in groundwater at a fire-training area at Wurtsmith Air Force Base, Michigan. *J. Environ. Monit.* 5, 341–345.
- Ny Teknik, 2014. Förhöjda halter PFAS hos Kallingeåren [WWW Document]. NyTeknik. URL http://www.nyteknik.se/nyheter/energi_miljo/miljo/article3815625.ece (accessed 5.28.15).

- Pan, G., Jia, C., Zhao, D., You, C., Chen, H., Jiang, G., 2009. Effect of cationic and anionic surfactants on the sorption and desorption of perfluorooctane sulfonate (PFOS) on natural sediments. *Environ. Pollut.* 157, 325–330.
- Pan, G., You, C., 2010. Sediment–water distribution of perfluorooctane sulfonate (PFOS) in Yangtze River Estuary. *Environ. Pollut.* 158, 1363–1367.
- Post, G.B., Louis, J.B., Lippincott, R.L., Procopio, N.A., 2013. Occurrence of Perfluorinated Compounds in Raw Water from New Jersey Public Drinking Water Systems. *Environ. Sci. Technol.* 47, 13266–13275.
- Rahman, M.F., Peldszus, S., Anderson, W.B., 2014. Behaviour and fate of perfluoroalkyl and polyfluoroalkyl substances (PFASs) in drinking water treatment: A review. *Water Res.* 50, 318–340.
- Rayne, S., Forest, K., 2009. Congener-specific organic carbon-normalized soil and sediment-water partitioning coefficients for the C₁ through C₈ perfluoroalkyl carboxylic and sulfonic acids. *J. Environ. Sci. Health Part A* 44, 1374–1387.
- Senevirathna, S.T.M.L.D., Tanaka, S., Fujii, S., Kunacheva, C., Harada, H., Shivakoti, B.R., Okamoto, R., 2010. A comparative study of adsorption of perfluorooctane sulfonate (PFOS) onto granular activated carbon, ion-exchange polymers and non-ion-exchange polymers. *Chemosphere* 80, 647–651.
- Tang, C.Y., Shiang Fu, Q., Gao, D., Criddle, C.S., Leckie, J.O., 2010. Effect of solution chemistry on the adsorption of perfluorooctane sulfonate onto mineral surfaces. *Water Res.* 44, 2654–2662.
- Wang, F., Liu, C., Shih, K., 2012. Adsorption behavior of perfluorooctanesulfonate (PFOS) and perfluorooctanoate (PFOA) on boehmite. *Chemosphere* 89, 1009–1014.
- Wang, Z., MacLeod, M., Cousins, I., T., Scheringer, M., Hungerbühler, K., 2011. Using COSMOtherm to predict physicochemical properties of poly- and perfluorinated alkyl substances (PFASs). *Environ. Chem.* 389–398.
- You, C., Jia, C., Pan, G., 2010. Effect of salinity and sediment characteristics on the sorption and desorption of perfluorooctane sulfonate at sediment-water interface. *Environ. Pollut.* 158, 1343–1347.
- Zareitalabad, P., Siemens, J., Hamer, M., Amelung, W., 2013. Perfluorooctanoic acid (PFOA) and perfluorooctanesulfonic acid (PFOS) in surface waters, sediments, soils and wastewater – A review on concentrations and distribution coefficients. *Chemosphere* 91, 725–732.

APPENDIX

Appendix I

Initial Concentrations in the Soil Suspensions

Determined initial concentrations for the Gustafsson et al., 2014 experiment of 1 g soil to 30 mL solution (Gustafsson et al., 2014b).

Parameter ^a	Value
Active humic acid (g L ⁻¹)	1.935
Active fulvic acid (g L ⁻¹)	0.645
Ca ²⁺ (μmol L ⁻¹)	662
Mg ²⁺ (μmol L ⁻¹)	136
K ⁺ (μmol L ⁻¹)	120
Mn ²⁺ (μmol L ⁻¹)	31.5
Al ³⁺ (μmol L ⁻¹)	228
Fe ³⁺ (μmol L ⁻¹)	35
Cr(OH) ₂ ⁺ (μmol L ⁻¹)	0.02
Cu ²⁺ (μmol L ⁻¹)	0.63

^a For cations the concentrations shown are geochemically active concentrations before any additions. For extraction methods see text.

Appendix II

Analysis results for dissolved organic carbon on filtered samples, from ALS Scandinavia AB.

Sample		DOC (mg L-1)	Uncertainty^a (+/-)
Al pH 3	a	72.6	14.6
Al pH 4	a	53	10.6
Al pH 5	a	65.8	13.2
Al pH 6	a	103	20.6
Al pH 3	b	68.3	13.7
Al pH 4	b	52.4	10.5
Al pH 5	b	72.4	14.5
Al pH 6	b	113	22.5
Ca pH 3 [5 mM]	a	68.6	13.7
Ca pH 4 [5 mM]	a	69.5	13.9
Ca pH 5 [5 mM]	a	38.4	7.69
Ca pH 6 [5 mM]	a	53.7	10.7
Ca pH 3 [5 mM]	b	75.6	15.1
Ca pH 4 [5 mM]	b	75.4	15.1
Ca pH 5 [5 mM]	b	34.2	0.85
Ca pH 6 [5 mM]	b	48.4	9.68
Ca pH 3 [3 mM]	a	65.5	13.1
Ca pH 4 [3 mM]	a	27.3	5.45
Ca pH 5 [3 mM]	a	43.9	8.78
Ca pH 6 [3 mM]	a	77.3	15.4
Ca pH 3 [3 mM]	b	75	15
Ca pH 4 [3 mM]	b	32.8	6.57
Ca pH 5 [3 mM]	b	44.7	8.94
Ca pH 6 [3 mM]	b	82.4	16.5
Na pH 3	a	67	13.4
Na pH 4	a	31.9	6.38
Na pH 5	a	43.4	8.67
Na pH 6	a	131	26.2
Na pH 3	b	71.1	14.2
Na pH 4	b	39.7	7.95
Na pH 5	b	56.9	11.4
Na pH 6	b	139	27.7

^a Corresponds to confidence level of 95%

Appendix III

Input and output Visual MINTEQ

Sample	INPUT												OUTPUT
	pH	Mg	Fe	Mn	K	DOC	FA solid	HA	Al	Ca	Na	NO ₃	Net charge
	(mM)	(mM)	(mM)	(mM)	(mM)	(mg L ⁻¹)	(g L ⁻¹)	(g L ⁻¹)	(mM)	(mM)	(mM)	(mM)	(mol L ⁻¹)
Na pH 3	3.1	0.15	0.04	0.03	0.13	69.1	0.54	2.04	0.24	0.71	10	12	-0.00121
Na pH 4	4.2	0.15	0.04	0.03	0.13	35.8	0.61	2.04	0.24	0.71	11	10	-0.00254
Na pH 5	4.9	0.15	0.04	0.03	0.13	50.2	0.58	2.04	0.24	0.71	12	10	-0.00357
Na pH 6	5.8	0.15	0.04	0.03	0.13	135	0.41	2.04	0.24	0.71	16	10	-0.00444
Ca pH 3 [5 mM]	2.9	0.15	0.04	0.03	0.13	72.1	0.54	2.04	0.24	5.71	4	16	-0.00105
Ca pH 4 [5 mM]	3.8	0.15	0.04	0.03	0.13	72.5	0.53	2.04	0.24	5.71	6	14	-0.00151
Ca pH 5 [5 mM]	4.6	0.15	0.04	0.03	0.13	36.3	0.61	2.04	0.24	5.71	9	14	-0.00167
Ca pH 6 [5 mM]	5.2	0.15	0.04	0.03	0.13	51.1	0.58	2.04	0.24	5.71	12	14	-0.00163
Ca pH 3 [3 mM]	2.9	0.15	0.04	0.03	0.13	70.3	0.54	2.04	0.24	3.71	4	12	-0.00104
Ca pH 4 [3 mM]	3.9	0.15	0.04	0.03	0.13	30.1	0.62	2.04	0.24	3.71	6	10	-0.00170
Ca pH 5 [3 mM]	4.9	0.15	0.04	0.03	0.13	44.3	0.59	2.04	0.24	3.71	9	10	-0.00199
Ca pH 6 [3 mM]	5.6	0.15	0.04	0.03	0.13	79.9	0.52	2.04	0.24	3.71	12	10	-0.00229
Al pH 3	2.8	0.15	0.04	0.03	0.13	70.5	0.54	2.04	2.24	0.71	4	10	-0.00058
Al pH 4	4.0	0.15	0.04	0.03	0.13	52.7	0.57	2.04	2.24	0.71	9	10	-0.00084
Al pH 5	4.8	0.15	0.04	0.03	0.13	69.1	0.54	2.04	2.24	0.71	11	10	-0.00152
Al pH 6	5.7	0.15	0.04	0.03	0.13	108	0.46	2.04	2.24	0.71	14	10	-0.00267

Appendix IV

Average K_d and K_{oc} with standard deviation, for each of the cation-series ($NaNO_3$, $Ca(NO_3)_2$ (5 mM and 3 mM) and $Al(NO_3)_3$). (n = number of samples, 8 where nothing else specified)

	Log $K_d \pm SD$ [ml g ⁻¹]						Log $K_{oc} \pm SD$ [ml g ⁻¹]							
	Al	Ca [5 mM]	(n)	Ca [3 mM]	(n)	Na	(n)	Al	Ca [5 mM]	(n)	Ca [3 mM]	(n)	Na	(n)
PFBA	0.4 ± 0.1	-0.6 ± 0.8	(4)	-0.2 ± 0.5	(4)	-0.6 ± 0.7	(3)	0.7 ± 0.1	-0.3 ± 0.8	(4)	0.1 ± 0.5	(4)	-0.3 ± 0.7	(3)
PFPeA	0.6 ± 0.2	0.3 ± 0.2	(7)	0.4 ± 0.2		0.3 ± 0.3	(7)	0.9 ± 0.2	0.6 ± 0.2	(7)	0.7 ± 0.2		0.7 ± 0.3	(7)
PFHxA	0.8 ± 0.1	0.5 ± 0.2		0.3 ± 0.4		0.3 ± 0.4		1.2 ± 0.1	0.8 ± 0.2		0.6 ± 0.4		0.6 ± 0.4	
PFHpA	1.1 ± 0.2	0.9 ± 0.2		0.7 ± 0.3		0.8 ± 0.2		1.5 ± 0.2	1.3 ± 0.2		1.1 ± 0.3		1.1 ± 0.2	
PFOA	1.7 ± 0.3	1.5 ± 0.2		1.3 ± 0.4		1.2 ± 0.3		2.1 ± 0.3	1.8 ± 0.2		1.6 ± 0.4		1.6 ± 0.3	
PFNA	2.6 ± 0.4	2.5 ± 0.2		2.1 ± 0.4		2.1 ± 0.5		3.0 ± 0.4	2.8 ± 0.2		2.5 ± 0.4		2.4 ± 0.5	
PFDA	3.6 ± 0.4	4.0 ± 0.6		3.6 ± 0.3		3.4 ± 0.3		3.9 ± 0.4	4.3 ± 0.6		3.9 ± 0.3		3.8 ± 0.3	
PFUnDA	3.9 ± 0.7	4.0 ± 0.6		4.1 ± 0.7		3.7 ± 0.5		4.3 ± 0.7	4.4 ± 0.6		4.4 ± 0.7		4.1 ± 0.5	
PFDoDA	3.7 ± 0.7	3.7 ± 0.7		3.7 ± 0.6		3.4 ± 0.4		4.1 ± 0.7	4.1 ± 0.7		4.0 ± 0.6		3.7 ± 0.4	
PFTeDA	3.8 ± 0.8	3.8 ± 0.8		3.7 ± 0.6		3.5 ± 0.5		4.2 ± 0.8	4.1 ± 0.8		4.0 ± 0.6		3.9 ± 0.5	
FOSA	4.3 ± 0.7	4.3 ± 0.5		4.1 ± 0.5		4.2 ± 0.5		4.6 ± 0.7	4.7 ± 0.5		4.5 ± 0.5		4.5 ± 0.5	
PFBS	0.5 ± 1.1	0.2 ± 0.4	(2)	0.2 ± 0.2	(5)	0.4 ± 0.7	(3)	0.9 ± 1.1	0.6 ± 0.4	(2)	0.6 ± 0.2	(5)	0.8 ± 0.7	(3)
PFHxS	2.6 ± 0.5	1.5 ± 0.0		1.2 ± 0.2		1.3 ± 0.4		3.0 ± 0.5	1.9 ± 0.0		1.6 ± 0.2		1.7 ± 0.4	
PFOS	3.7 ± 0.3	4.0 ± 0.5		3.8 ± 0.4		3.5 ± 0.2		4.0 ± 0.3	4.4 ± 0.5		4.1 ± 0.4		3.9 ± 0.2	

Appendix V

Analysis results for PFASs detected in liquid phase (ng L^{-1}), for all samples. Volume refers to sample volume that underwent SPE.

Sample	volume [L]	PFBA	PFPea	PFHxA	PFHpA	PFOA	PFNA	PFDA	PFUnDA	PFDDa	PFTeDa	FOSA	PFBS	PFHxS	PFOS
Blank	0.021	0	0	0	0	0	0	0	0	0	0	0	0	0	0
Blank	0.019	0	0	0	0	0	0	0	0	0	0	0	0	0	0
Blank+PFASa	a 0.021	879	830	923	876	878	883	761	411	62	3	10	871	800	483
Blank+PFASa	b 0.020	880	831	916	872	878	880	784	365	41	1	4	930	763	485
Al pH 3	a 0.011	797	705	711	505	187	27	2	2	2	0	0	951	142	3
Al pH 4	a 0.011	795	731	742	575	254	35	5	7	1	1	4	721	12	2
Al pH 5	a 0.010	811	705	765	599	317	63	6	1	12	1	4	541	18	5
Al pH 6	a 0.011	815	647	815	682	504	189	15	11	21	13	7	699	166	7
Al pH 3	b 0.011	830	756	718	504	170	21	2	0	0	0	0	954	43	3
Al pH 4	b 0.011	830	750	763	597	282	44	8	0	1	1	0	678	23	2
Al pH 5	b 0.010	820	729	772	638	364	87	13	15	18	10	6	656	53	11
Al pH 6	b 0.011	830	645	796	668	480	194	25	13	26	15	7	672	107	6
Ca pH 3 [5 mM]	a 0.011	842	740	774	578	294	55	7	1	2	1	1	1144	341	1
Ca pH 4 [5 mM]	a	-	-	-	-	-	-	-	-	-	-	-	-	-	-
Ca pH 5 [5 mM]	a 0.010	879	762	858	699	501	107	1	1	5	3	0	1022	383	0
Ca pH 6 [5 mM]	a 0.010	852	714	848	704	508	114	13	10	19	11	5	872	365	6
Ca pH 3 [5 mM]	b 0.011	881	778	800	579	281	43	1	0	0	0	0	1148	343	2
Ca pH 4 [5 mM]	b 0.010	883	786	863	714	416	64	1	1	3	1	1	1091	348	1
Ca pH 5 [5 mM]	b 0.011	907	765	857	724	504	102	9	8	12	7	3	1035	381	5
Ca pH 6 [5 mM]	b 0.010	889	734	865	713	519	112	6	6	15	13	4	927	370	3
Ca pH 3 [3 mM]	a 0.019	853	718	775	571	281	43	2	0	0	0	0	1142	342	1
Ca pH 4 [3 mM]	a 0.017	837	732	853	712	523	174	5	1	3	1	1	892	477	2
Ca pH 5 [3 mM]	a 0.011	913	781	883	815	595	259	14	4	6	4	3	1295	536	4
Ca pH 6 [3 mM]	a 0.010	911	738	901	781	685	319	24	19	26	13	8	921	550	13
Ca pH 3 [3 mM]	b 0.019	867	717	773	548	284	46	5	0	5	2	1	892	345	2
Ca pH 4 [3 mM]	b 0.019	878	758	880	713	515	165	5	2	5	3	3	1143	510	3
Ca pH 5 [3 mM]	b 0.010	907	775	886	766	621	242	11	6	12	8	2	933	504	7
Ca pH 6 [3 mM]	b 0.010	922	745	910	786	614	297	9	8	17	12	4	922	517	5
Na pH 3	a 0.010	862	768	794	590	313	46	21	20	21	1	1	1129	331	15
Na pH 4	a 0.010	867	758	841	708	543	195	6	3	7	2	2	961	505	6
Na pH 5	a 0.010	881	757	880	751	660	321	7	5	11	8	2	940	555	5
Na pH 6	a 0.010	887	677	874	755	681	377	12	10	22	16	7	853	588	7
Na pH 3	b 0.010	903	788	826	627	304	221	6	0	7	3	0	1120	284	3
Na pH 4	b 0.010	938	852	919	769	582	221	6	2	7	1	1	1039	522	6
Na pH 5	b 0.010	889	755	881	761	634	324	9	6	12	6	3	1008	555	6
Na pH 6	b 0.010	905	683	876	749	590	304	37	8	19	13	6	670	171	5

Appendix VI

Analysis results for PFASs in solid phase (ng g⁻¹) for all samples, using (Eq 2).

Sample	Soil weight [g]	PFBA	PFPeA	PFHxA	PFHpA	PFOA	PFNA	PFDA	PFUnDA	PFDoDA	PFTeDA	FOSA	PFBS	PFHxS	PFOS
Al pH 3	a 1.34	2.5	3.0	6.4	10.8	19.9	25.9	26.8	23.9	23.6	13.4	24.8	0.1	18.3	18.9
Al pH 4	a 1.33	2.6	2.3	5.5	8.7	17.9	25.7	26.7	24.0	23.7	13.4	24.8	7.0	22.2	19.0
Al pH 5	a 1.33	2.1	3.0	4.8	8.0	16.0	24.8	26.7	23.8	23.4	13.3	24.7	12.4	22.0	18.9
Al pH 6	a 1.34	2.0	4.8	3.3	5.5	10.4	21.0	26.4	23.7	23.1	13.0	24.6	7.7	17.6	18.8
Al pH 3	b 1.34	1.6	1.5	6.2	10.8	20.4	26.1	26.8	24.0	23.7	13.4	24.8	0.0	21.3	18.9
Al pH 4	b 1.33	1.6	1.7	4.9	8.0	17.1	25.4	26.7	24.0	23.7	13.4	24.8	8.3	21.9	18.9
Al pH 5	b 1.34	1.9	2.3	4.6	6.8	14.6	24.1	26.5	23.5	23.2	13.1	24.6	9.0	21.0	18.7
Al pH 6	b 1.34	1.6	4.9	3.9	5.9	11.1	20.9	26.1	23.6	22.9	13.0	24.6	8.5	19.4	18.8
Ca pH 3 [5 mM]	a 1.34	1.2	2.0	4.6	8.6	16.7	25.1	26.7	24.0	23.7	13.4	24.7	-5.7	12.4	19.0
Ca pH 4 [5 mM]	a 1.33	0.1	1.3	2.0	5.0	10.5	23.5	26.9	24.0	23.6	13.3	24.8	-2.0	11.1	19.0
Ca pH 5 [5 mM]	a 1.33	0.9	2.8	2.4	4.8	10.3	23.3	26.5	23.7	23.2	13.1	24.6	2.5	11.6	18.8
Ca pH 6 [5 mM]	b 1.33	0.0	0.9	3.8	8.6	17.1	25.4	26.8	24.0	23.7	13.4	24.8	-5.8	12.3	19.0
Ca pH 4 [5 mM]	b 1.33	0.0	0.6	1.9	4.5	13.0	24.8	26.9	24.0	23.6	13.4	24.7	-4.1	12.1	19.0
Ca pH 5 [5 mM]	b 1.33	-0.8	1.2	2.1	4.2	10.4	23.7	26.6	23.8	23.4	13.2	24.7	-2.4	11.2	18.9
Ca pH 6 [5 mM]	b 1.33	-0.2	2.2	1.8	4.6	10.0	23.3	26.7	23.8	23.3	13.0	24.6	0.8	11.5	18.9
Ca pH 3 [3 mM]	a 1.33	0.9	2.6	4.5	8.8	17.1	25.4	26.8	24.0	23.7	13.4	24.8	-5.6	12.3	19.0
Ca pH 4 [3 mM]	a 1.33	1.4	2.2	2.2	4.6	9.8	21.5	26.7	24.0	23.6	13.4	24.7	1.9	8.3	19.0
Ca pH 5 [3 mM]	a 1.33	-0.9	0.8	1.3	1.5	7.7	19.0	26.5	23.9	23.5	13.3	24.7	-10.2	6.5	18.9
Ca pH 6 [3 mM]	a 1.34	-0.9	2.1	0.8	2.5	5.0	17.2	26.2	23.4	22.9	13.0	24.5	1.0	6.1	18.6
Ca pH 3 [3 mM]	b 1.34	0.5	2.7	4.6	9.5	17.0	25.3	26.7	24.0	23.7	13.4	24.7	1.9	12.2	18.9
Ca pH 4 [3 mM]	b 1.33	0.1	1.5	1.4	4.5	10.1	21.8	26.7	23.9	23.6	13.3	24.7	-5.6	7.3	18.9
Ca pH 5 [3 mM]	b 1.33	-0.7	0.9	1.2	2.9	6.9	19.5	26.6	23.8	23.4	13.2	24.7	0.7	7.5	18.8
Ca pH 6 [3 mM]	b 1.34	-1.2	1.8	0.5	2.4	5.3	17.8	26.6	23.7	23.2	13.0	24.6	1.0	7.1	18.9
Na pH 3	a 1.33	0.6	1.2	4.0	8.2	16.1	25.3	26.2	23.4	23.1	13.4	24.7	-5.2	12.6	18.5
Na pH 4	a 1.33	0.4	1.5	2.5	4.7	9.2	20.9	26.7	23.9	23.5	13.4	24.7	-0.2	7.4	18.8
Na pH 5	a 1.33	0.0	1.5	1.4	3.4	5.7	17.1	26.7	23.8	23.4	13.2	24.7	0.5	5.9	18.9
Na pH 6	a 1.33	-0.1	3.9	1.6	3.3	5.1	15.4	26.5	23.7	23.1	12.9	24.6	3.0	4.9	18.8
Na pH 3	b 1.33	-0.6	0.6	3.0	7.1	16.4	26.1	26.7	24.0	23.7	13.4	24.8	-5.0	14.1	18.9
Na pH 4	b 1.33	-1.7	-1.4	0.2	2.9	8.1	20.1	26.7	23.9	23.5	13.3	24.7	-2.5	6.9	18.8
Na pH 5	b 1.33	-0.2	1.6	1.4	3.1	6.5	17.0	26.6	23.8	23.4	13.2	24.7	-1.6	5.9	18.8
Na pH 6	b 1.33	-0.7	3.7	1.5	3.5	7.8	17.6	25.8	23.7	23.2	13.0	24.6	8.5	17.4	18.9

Appendix VII

Analysis results for K_d (mL g^{-1}) for all samples, using (Eq 4).

Sample	PFBA	PFPeA	PFHxA	PFHpA	PFOA	PFNA	PFDA	PFUnDA	PFDoDA	PFTeDA	FOSA	PFBS	PFHxS	PFOS
Al pH 3	0.5	0.6	1.0	1.3	2.0	3.0	4.1	4.1	4.0	4.9	5.1	-0.9	2.1	3.8
Al pH 4	0.5	0.5	0.9	1.2	1.8	2.9	3.7	4.3	4.3	4.2	4.8	1.0	3.3	4.0
Al pH 5	0.4	0.6	0.8	1.1	1.7	2.6	3.6	3.5	3.3	3.5	3.8	1.4	3.1	3.6
Al pH 6	0.4	0.9	0.6	0.9	1.3	2.0	3.2	3.3	3.0	3.0	3.6	1.0	2.0	3.5
Al pH 3	0.3	0.3	0.9	1.3	2.1	3.1	4.2	5.0	4.8	4.7	5.2	-1.5	2.7	3.8
Al pH 4	0.3	0.4	0.8	1.1	1.8	2.8	3.5	4.8	4.2	4.4	4.8	1.1	3.0	3.9
Al pH 5	0.4	0.5	0.8	1.0	1.6	2.4	3.3	3.2	3.1	3.1	3.6	1.1	2.6	3.2
Al pH 6	0.3	0.9	0.7	0.9	1.4	2.0	3.0	3.2	2.9	2.9	3.5	1.1	2.3	3.5
Ca pH 3 [15 mM]	0.2	0.4	0.8	1.2	1.8	2.7	3.6	4.4	4.1	4.3	4.5		1.6	4.3
Ca pH 4 [15 mM]	-1.0	0.2	0.4	0.9	1.3	2.3	4.7	4.2	3.7	3.6	4.7		1.5	4.9
Ca pH 5 [15 mM]	0.0	0.6	0.4	0.8	1.3	2.3	3.3	3.4	3.1	3.1	3.7	0.5	1.5	3.5
Ca pH 3 [15 mM]	-1.6	0.0	0.7	1.2	1.8	2.8	4.3	4.9	5.0	5.1	4.8		1.6	4.0
Ca pH 4 [15 mM]	-0.1	0.3	0.3	0.8	1.5	2.6	4.7	4.3	3.9	4.0	4.6		1.5	4.2
Ca pH 5 [15 mM]	0.2	0.2	0.4	0.8	1.3	2.4	3.5	3.5	3.3	3.3	4.0		1.5	3.6
Ca pH 6 [15 mM]	0.5	0.5	0.3	0.8	1.3	2.3	3.6	3.6	3.2	3.0	3.8	0.0	1.5	3.8
Ca pH 3 [13 mM]	0.0	0.6	0.8	1.2	1.8	2.8	4.1	5.4	4.7	4.7	5.0		1.6	4.5
Ca pH 4 [13 mM]	0.2	0.5	0.4	0.8	1.3	2.1	3.7	4.4	3.9	4.2	4.4	0.3	1.2	4.0
Ca pH 5 [13 mM]	0.0	0.0	0.2	0.3	1.1	1.9	3.3	3.8	3.6	3.5	4.0		1.1	3.7
Ca pH 6 [13 mM]	0.4	0.4	-0.1	0.5	0.9	1.7	3.0	3.1	2.9	3.0	3.5	0.0	1.0	3.2
Ca pH 3 [13 mM]	-0.3	0.6	0.8	1.2	1.8	2.7	3.8	4.7	4.2	3.8	4.5	0.3	1.5	3.9
Ca pH 4 [13 mM]	-0.9	0.3	0.2	0.8	1.3	2.1	3.7	4.1	3.7	3.7	3.9		1.2	3.4
Ca pH 5 [13 mM]	0.1	0.1	0.1	0.6	1.0	1.9	3.4	3.6	3.3	3.2	4.1	-0.2	1.2	3.8
Ca pH 6 [13 mM]	0.4	0.4	-0.3	0.5	0.9	1.8	3.5	3.5	3.1	3.0	3.8	0.0	1.1	3.6
Na pH 3	-0.1	0.2	0.7	1.1	1.7	2.7	3.1	3.1	3.0	4.0	4.6		1.6	3.1
Na pH 4	-0.3	0.3	0.5	0.8	1.2	2.0	3.7	3.9	3.5	3.9	4.2		1.2	3.5
Na pH 5	-1.4	0.3	0.2	0.7	0.9	1.7	3.6	3.7	3.3	3.2	4.0	-0.3	1.0	3.6
Na pH 6	0.8	0.8	0.3	0.6	0.9	1.6	3.3	3.4	3.0	2.9	3.5	0.6	0.9	3.4
Na pH 3	-0.1	0.1	0.6	1.1	1.7	3.1	3.7	4.9	4.2	4.3	5.2		1.7	3.9
Na pH 4	-0.6	0.6	0.6	0.6	1.1	2.0	3.6	4.0	3.5	3.7	4.3		1.1	3.5
Na pH 5	0.3	0.3	0.2	0.6	1.0	1.7	3.5	3.6	3.3	3.3	3.9		1.0	3.5
Na pH 6	0.7	0.7	0.2	0.7	1.1	1.8	2.8	3.5	3.1	3.0	3.6	1.1	2.0	3.6